SYRU/DECE/TR-86/4

ELECTROMAGNETIC PENETRATION INTO A CONDUCTING CIRCULAR CYLINDER THROUGH A NARROW SLOT, TM CASE

Interim Technical Report No. 6

by

Joseph R. Mautz

Roger F. Harrington

December 1986

Department of
Electrical and Computer Engineering
Syracuse University
Syracuse, New York 13210

Contract No. DAAG29-84-K-0078

Prepared for

ARMY RESEARCH OFFICE
RESEARCH TRIANGLE PARK
NORTH CAROLINA 27709

SYRU/DECE/TR-86/4

ELECTROMAGNETIC PENETRATION INTO A CONDUCTING CIRCULAR CYLINDER THROUGH A NARROW SLOT, TM CASE

Interim Technical Report No. 6

by

Joseph R. Mautz

Roger F. Harrington

December 1986

Department of
Electrical and Computer Engineering
Syracuse University
Syracuse, New York 13210

Contract No. DAAG29-84-K-0078

Approved for public release; distribution unlimited

Prepared for

ARMY RESEARCH OFFICE
RESEARCH TRIANGLE PARK
NORTH CAROLINA 27709

AD-A176483

REPORT DOCUMENTATION PAGE

READ INSTRUCTIONS BEFORE COMPLETING FORM

1. REPORT NUMBER: ARO 21378.8-EL
2. GOVT ACCESSION NO.
3. RECIPIENT'S CATALOG NUMBER

4. TITLE (and Subtitle): ELECTROMAGNETIC PENETRATION INTO A CONDUCTING CIRCULAR CYLINDER THROUGH A NARROW SLOT, TM CASE
5. TYPE OF REPORT & PERIOD COVERED: Interim Technical Report #6
6. PERFORMING ORG. REPORT NUMBER

7. AUTHOR(s):
Joseph R. Mautz
Roger F. Harrington
8. CONTRACT OR GRANT NUMBER(s): DAAG29-84-K-0078

9. PERFORMING ORGANIZATION NAME AND ADDRESS:
Department of Electrical & Computer Engineering
Syracuse University
Syracuse, New York 13244-1240
10. PROGRAM ELEMENT, PROJECT, TASK AREA & WORK UNIT NUMBERS

11. CONTROLLING OFFICE NAME AND ADDRESS:
U.S. Army Research Office
Post Office Box 12211
Research Triangle Park, NC 27709
12. REPORT DATE: December 1986
13. NUMBER OF PAGES

14. MONITORING AGENCY NAME & ADDRESS (if different from Controlling Office)
15. SECURITY CLASS. (of this report): UNCLASSIFIED
15a. DECLASSIFICATION/DOWNGRADING SCHEDULE

16. DISTRIBUTION STATEMENT (of this Report)

Approved for public release; distribution unlimited

17. DISTRIBUTION STATEMENT (of the abstract entered in Block 20, if different from Report)

NA

18. SUPPLEMENTARY NOTES

The view, opinions, and/or findings contained in this report are those of the author(s) and should not be construed as an official Department of the Army position, policy, or decision, unless so designated by other documentation.

19. KEY WORDS (Continue on reverse side if necessary and identify by block number)

Aperture problems
Circular cylinder
Electromagnetic penetration
Magnetic current
Numerical solution
Resonance

20. ABSTRACT (Continue on reverse side if necessary and identify by block number)

A procedure is presented for calculating the electromagnetic field in the vicinity of an infinitesimally thin conducting circular cylindrical shell with an infinitely long slot illuminated by a TM plane wave. This field is the short-circuit field plus the field due to the slot. The short-circuit field is the field that would exist if there were no slot. The field due to the slot stems from the axial electric field in the slot. Approximated by a linear combination of expansion functions that satisfy the edge conditions,

20. ABSTRACT

the latter field is determined by testing the equation of continuity of the tangential magnetic field in the slot with non-negative powers of ϕ where $|\phi|$ is the angular distance from the center of the slot.

Alternative expansion functions are introduced to preserve the accuracy of the solution in the vicinity of an internal resonance. Containing the resonant electric field, the first alternative expansion function is normalized so that its tangential magnetic field remains finite as the resonant frequency is approached. The rest of the alternative expansion functions are orthogonal to the resonant electric field.

Accession For	
NTIS GRA&I	☒
DTIC TAB	☐
Unannounced	☐
Justification	
By	
Distribution/	
Availability Codes	
Dist	Avail and/or Special
A-1	

CONTENTS

I. INTRODUCTION

Scattering of a TM electromagnetic wave by a conducting circular cylindrical shell with an infinitely long slot can be computed by a numerical solution of the E-field integral equation [1], [2] or by the pseudo-image method [3], [4]. If computations are done in single precision with seven significant figures, the method presented in [1] and [2] fails to accurately determine the field inside the cylinder when the slot is so narrow that the magnitude of this field is less than one millionth of the magnitude of the incident field. The incident field is the field that would exist if the cylinder were absent. The pseudo-image method can be used to accurately determine such an extremely small interior field, provided that the frequency is not close to a resonant frequency of the associated cavity. The associated cavity is the cavity enclosed by the complete cylindrical surface. The complete cylindrical surface is the conducting shell with the slot covered by a conducting surface whose radius of curvature is the same as that of the shell. Unfortunately, the pseudo-image method fails when the frequency is close to a resonant frequency of the associated cavity.

Basic theoretical work was done by Rhodes [5]. Later, the problem was reduced to that of solving a singular integral equation [6]. More recently, Riemann-Hilbert problem techniques have been applied to both TM and TE excited shells [7] and to the TE excited shell [8]-[10]. Unfortunately, we have not been able to extract numerical data from [5]-[10] for the problem of the TM excited circular cylindrical shell with a very narrow slot when the frequency is close to a resonant frequency of the associated cavity.

The formulation presented in this report gives an accurate numerical solution to the problem mentioned in the previous sentence. This formulation is the generalized network formulation for aperture problems [11] with the matrix elements evaluated by replacing each expansion function by a very large but finite number of terms in its Fourier series. To obtain a matrix that remains well-conditioned as the frequency approaches the resonant frequency of the associated cavity, we choose expansion functions so that the magnetic field of only one of them contains the resonant magnetic field. At present, we are unable to numerically solve the more general problem of an arbitrary (non-circular) cylindrical shell because the resonant frequencies and modes of the associated cavity are not known.

II. MATHEMATICAL FORMULATION

An infinitesimally thin, perfectly conducting cylindrical shell of radius a having a slit aperture of half angle ϕ_o is illuminated by a TM polarized plane wave. In terms of the polar coordinates (ρ,ϕ,z), the equation of the shell is $(\rho=a,\ \phi_o \leq \phi \leq 2\pi - \phi_o)$ and the incident electric field $\underline{E}^i$ is taken to be

$$\underline{E}^i = \underline{u}_z\, e^{jk\rho\cos(\phi-\alpha)} \tag{1}$$

where a time factor $e^{j\omega t}$ has been assumed and suppressed. See Fig. 1. The incident electric field is the electric field that would exist if the shell were absent. In (1), $\underline{u}_z$ is the unit vector in the z direction, α is the angle of the direction from which the incident wave comes, and $k = \omega\sqrt{\mu\varepsilon}$ is the wave number where μ and ε are, respectively, the permeability and permittivity of the medium surrounding the shell. Our objective

is to find the electric and magnetic fields everywhere in Fig. 1.

We close aperture with an infinitely thin curved conducting strip whose equation is ($\rho = a$, $|\phi| \leq \phi_o$) and, as shown in Fig. 2, we place the magnetic current $\underline{M}$ on the right-hand side of the closed aperture and $-\underline{M}$ on the left-hand side of the closed aperture. These magnetic currents restore the tangential electric field in the aperture. The situation in Fig. 2 will be equivalent to that in Fig. 1 if the tangential magnetic field is continuous across the closed aperture. Thus, since the magnetic field of a TM wave is transverse, we require that

$$H_\phi^b(-\underline{M}) = H_\phi^a(\underline{M}) + H_\phi^{sc}, \quad \begin{cases} \rho = a \\ |\phi| \leq \phi_o \end{cases} \tag{2}$$

where the subscript ϕ denotes the ϕ component. Here, $\underline{H}^b(-\underline{M})$ is the magnetic field due to $-\underline{M}$ placed on the region b side of the closed aperture in Fig. 2, $\underline{H}^a(\underline{M})$ is the magnetic field due to $\underline{M}$ placed on the region a side of the closed aperture, and $\underline{H}^{sc}$ is the magnetic field that would exist if the incident wave impinged on the conducting shell with its aperture closed, i.e., on the conducting circular cylinder of radius a. Region a is the region for which $\rho \geq a$. Region b is the region for which $\rho \leq a$.

Equation (2) is recast as

$$H_\phi^b(-\underline{M}) - H_\phi^a(\underline{M}) = H_\phi^{sc}, \quad \begin{cases} \rho = a \\ |\phi| \leq \phi_o \end{cases} \tag{3}$$

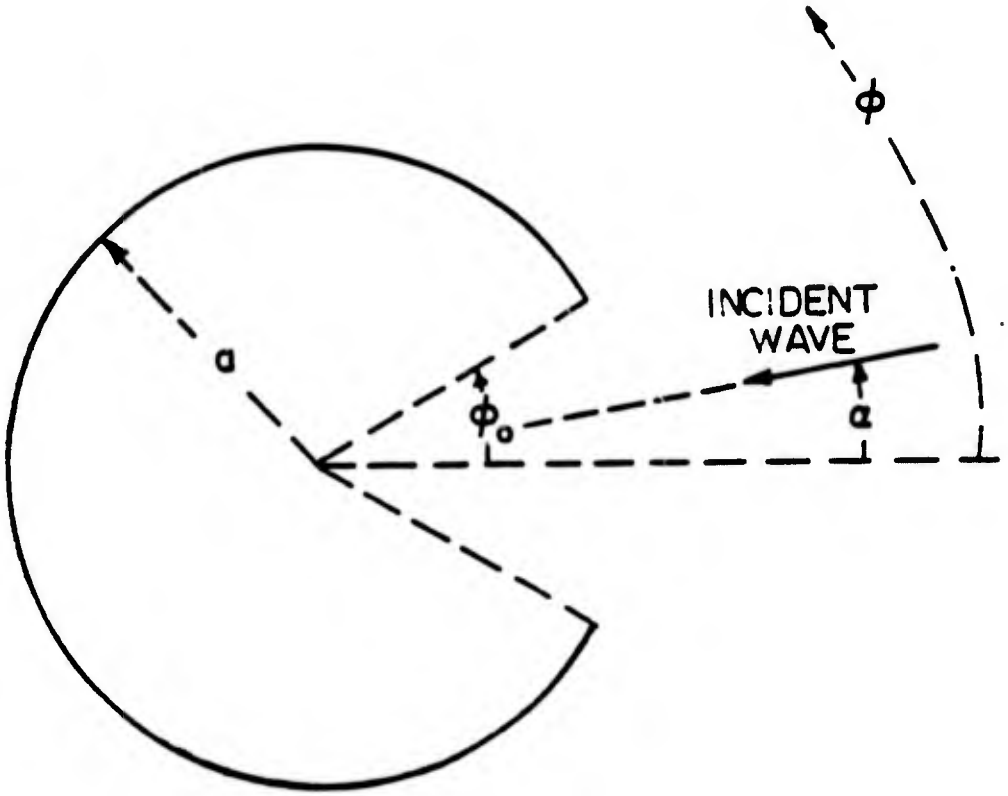

Fig. 1. The geometry.

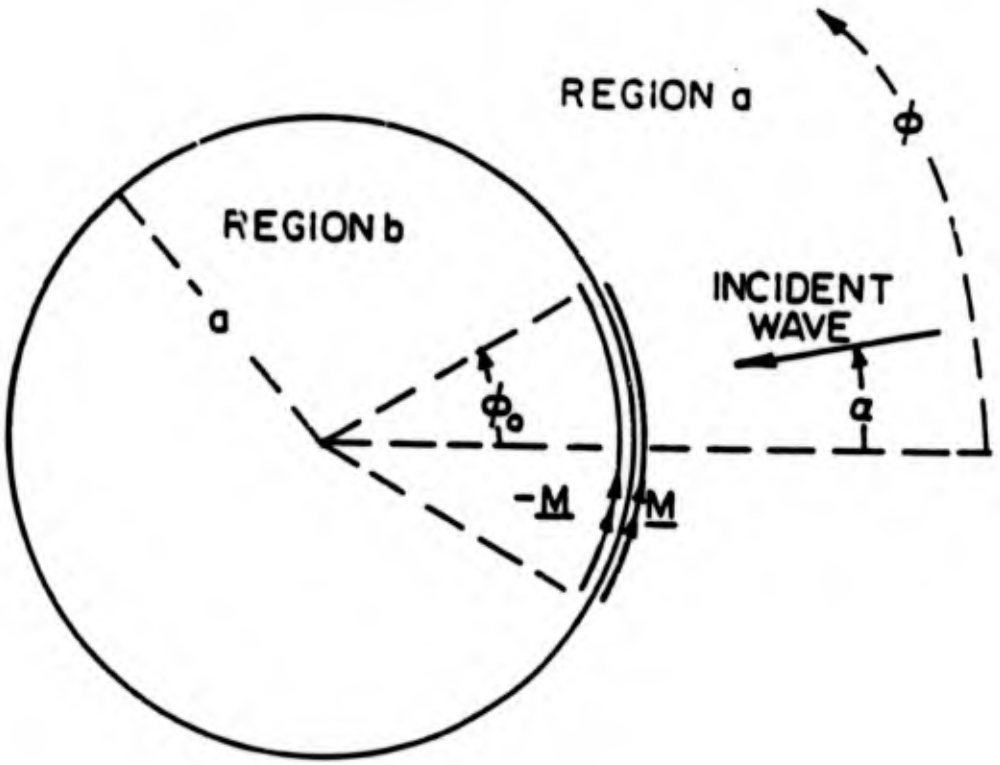

Fig. 2. Equivalent situation.

We let

$$\underline{M} = \underline{u}_\phi (M^e + M^o) \tag{4}$$

where M^e is even in ϕ, M^o is odd in ϕ, and $\underline{u}_\phi$ is the unit vector in the ϕ direction. Because the magnetic fields due to $\underline{u}_\phi M^e$ are even in ϕ and those due to $\underline{u}_\phi M^o$ are odd in ϕ, (3) decomposes into

$$H_\phi^b(-\underline{u}_\phi M^e) - H_\phi^a(\underline{u}_\phi M^e) = H_\phi^{sce}, \quad \begin{cases} \rho=a \\ |\phi| \leq \phi_o \end{cases} \tag{5}$$

and

$$H_\phi^b(-\underline{u}_\phi M^o) - H_\phi^a(\underline{u}_\phi M^o) = H_\phi^{sco}, \quad \begin{cases} \rho=a \\ |\phi| \leq \phi_o \end{cases} \tag{6}$$

where H_ϕ^{sce} is the even part of H_ϕ^{sc} and H_ϕ^{sco} is the odd part of H_ϕ^{sc}.

Seeking an approximate numerical solution to (5), we let

$$M^e = \sum_{j=1}^{4} V_j^e M_j^e \tag{7}$$

where

$$M_j^e = \begin{cases} (\phi/\phi_o)^{2j-2} \sqrt{1 - (\phi/\phi_o)^2}, & |\phi| \leq \phi_o \\ 0, & \text{otherwise} \end{cases} \tag{8}$$

The expansion functions (8) are reasonable because the equivalent magnetic current for a narrow, but infinitely long slot in a planar conducting screen of infinite extent excited by a wave TM to the slot axis has $\sqrt{w^2 - x^2}$ and $x\sqrt{w^2 - x^2}$ terms [12, eq. (17)] where w is one half of the slot width and $|x|$ is the distance from the center of the slot. Substitution of (7) into (5) gives

$$\sum_{j=1}^{4} V_j^e [H_\phi^b(-\underline{u}_\phi M_j^e) - H_\phi^a(\underline{u}_\phi M_j^e)] = H_\phi^{sce}, \quad \begin{cases} \rho=a \\ |\phi| \leq \phi_o \end{cases} \tag{9}$$

In (9), H_ϕ^a is the ϕ component of the magnetic field in region a of Fig. 3, and H_ϕ^b is the ϕ component of the magnetic field in region b

of Fig. 3. The fields in Fig. 3 are obtained by solving the boundary value problem in which E_z, the z component of electric field, is continuous at $\rho = a$ where it is given by

$$E_z = M_j^e \tag{10}$$

In terms of the elementary wave functions described in [13, Sec. 5-1], E_z is given by

$$\left.\begin{aligned} E_z^a &= \sum_{n=0}^{\infty} \frac{S_{jn}^e \, H_n^{(2)}(k\rho) \cos(n\phi)}{H_n^{(2)}(ka)} \\ E_z^b &= \sum_{n=0}^{\infty} \frac{S_{jn}^e \, J_n(k\rho) \cos(n\phi)}{J_n(ka)} \end{aligned}\right\} \tag{11}$$

where E_z^a is E_z in region a and E_z^b is E_z in region b. The coefficient S_{jn}^e is such that

$$M_j^e = \sum_{n=0}^{\infty} S_{jn}^e \cos(n\phi) \tag{12}$$

From (12), S_{jn}^e is the following integral over the source M_j^e.

$$S_{jn}^e = \frac{\varepsilon_n}{2\pi} \int_{-\phi_o}^{\phi_o} M_j^e(\phi) \cos(n\phi) \, d\phi \tag{13}$$

Here, ε_n is Neumann's number

$$\varepsilon_n = \begin{cases} 1, & n = 0 \\ 2 & n \geq 1 \end{cases} \tag{14}$$

Substitution of (8) into (13) gives

$$S_{jn}^e = \frac{\varepsilon_n}{2\pi} \int_{-\phi_o}^{\phi_o} (\phi/\phi_o)^{2j-2} \sqrt{1 - (\phi/\phi_o)^2} \cos(n\phi) \, d\phi \tag{15}$$

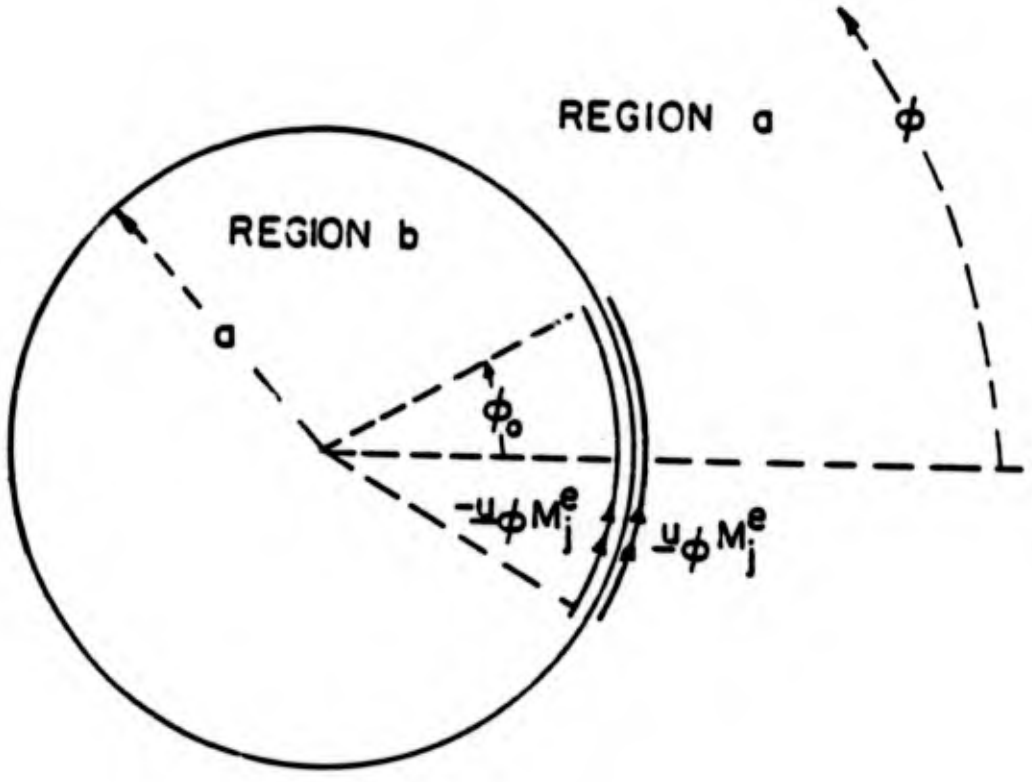

Fig. 3. Situation in which H_ϕ^a and H_ϕ^b of (9) exist.

The coefficient S^e_{jn} is evaluated in Appendix A.

It is evident from [13, eq. (5-18)] that

$$H_\phi^{a,b} = \frac{-j}{k\eta} \frac{\partial}{\partial \rho} E_z^{a,b} \tag{16}$$

where $\eta = \sqrt{\mu/\varepsilon}$ and "a,b" means either a or b. Of course, a denotes region a, and b denotes region b. Substitution of (11) into (16) gives

$$\left.\begin{aligned} H_\phi^a &= -\frac{j}{\eta} \sum_{n=0}^{\infty} \frac{S^e_{jn} H_n^{(2)'}(k\rho) \cos(n\phi)}{H_n^{(2)}(ka)} \\ H_\phi^b &= -\frac{j}{\eta} \sum_{n=0}^{\infty} \frac{S^e_{jn} J'_n(k\rho) \cos(n\phi)}{J_n(ka)} \end{aligned}\right\} \tag{17}$$

Using (17) and the Wronskian [13, eqs. (D-12) and (D-17)]

$$J_n(ka) H_n^{(2)'}(ka) - J'_n(ka) H_n^{(2)}(ka) = -\frac{2j}{\pi ka} \tag{18}$$

we obtain

$$[H_\phi^b - H_\phi^a]_{\rho=a} = \frac{2}{\pi\eta ka} \sum_{n=0}^{\infty} \frac{S^e_{jn} \cos(n\phi)}{J_n(ka) H_n^{(2)}(ka)} \tag{19}$$

which, when substituted into (9), gives

$$\frac{2}{\pi\eta ka} \sum_{j=1}^{4} V_j^e \left(\sum_{n=0}^{\infty} \frac{S^e_{jn} \cos(n\phi)}{J_n(ka) H_n^{(2)}(ka)} \right) = [H_\phi^{sce}]_{\rho=a}, \quad |\phi| \le \phi_o \tag{20}$$

It is evident from [13, eq. (5-109)] that

$$[H_\phi^{sc}]_{\rho=a} = \frac{2}{\pi\eta ka} \sum_{n=-\infty}^{\infty} \frac{j^n e^{jn(\phi-\alpha)}}{H_n^{(2)}(ka)} \tag{21}$$

The even part of (21) is given by

$$[H_\phi^{sce}]_{\rho=a} = \frac{4}{\pi\eta ka} \sum_{n=0}^{\infty} \frac{\varepsilon_n j^n \cos(n\alpha) \cos(n\phi)}{2H_n^{(2)}(ka)} \tag{22}$$

Substitution of (22) into (20) and subsequent multiplication by $\pi\eta ka/4$ give

$$\frac{1}{2} \sum_{j=1}^{4} V_j^e \left(\sum_{n=0}^{\infty} \frac{S_{jn}^e \cos(n\phi)}{J_n(ka)\, H_n^{(2)}(ka)} \right) = \sum_{n=0}^{\infty} \frac{\varepsilon_n j^n \cos(n\alpha) \cos(n\phi)}{2H_n^{(2)}(ka)}, \quad |\phi| \leq \phi_o \tag{23}$$

Seeking an approximate numerical solution to (6), we let

$$M^o = \sum_{j=1}^{4} V_j^o M_j^o \tag{24}$$

where

$$M_j^o = \begin{cases} (\phi/\phi_o)^{2j-1} \sqrt{1 - (\phi/\phi_o)^2}, & |\phi| \leq \phi_o \\ 0, & \text{otherwise} \end{cases} \tag{25}$$

Proceeding as in the development (9)-(23), we obtain

$$\frac{1}{2} \sum_{j=1}^{4} V_j^o \left(\sum_{n=1}^{\infty} \frac{S_{jn}^o \sin(n\phi)}{J_n(ka)\, H_n^{(2)}(ka)} \right) = \sum_{n=1}^{\infty} \frac{j^n \sin(n\alpha) \sin(n\phi)}{H_n^{(2)}(ka)}, \quad |\phi| \leq \phi_o \tag{26}$$

where

$$S_{jn}^o = \frac{1}{\pi} \int_{-\phi_o}^{\phi_o} (\phi/\phi_o)^{2j-1} \sqrt{1 - (\phi/\phi_o)^2} \sin(n\phi)\, d\phi \tag{27}$$

The coefficient S_{jn}^o is evaluated in Appendix A.

When the frequency is very close to a resonant frequency of the associated cavity, there is an integer p such that $|J_p(ka)|$ is extremely small. In this case, it can be seen by the following reasoning that any numerical method of solution of (23) will fail to accurately determine V_j^e. The four cos $(p\phi)$ terms on the left-hand side of (23) become so large that none of the other terms can be discerned. As a result, the only information that can be extracted from (23) is that

$$\sum_{j=1}^{4} V_j^e S_{jp}^e = 0 \tag{28}$$

This single equation is not sufficient to determine V_1^e, V_2^e, V_3^e, and V_4^e.

There should be no difficulty in solving (26) numerically when $|J_o(ka)|$ is very small because $J_o(ka)$ does not appear in (26). However, if $|J_p(ka)|$ is very small where p is a positive integer, then numerical solution of (26) will be just as difficult as that of (23).

III. ALTERNATIVE EXPANSION FUNCTIONS

In this section, the expansion functions are changed in order to eliminate the indeterminacy encountered in the last two paragraphs of Section II. If $|J_p(ka)|$ is extremely small, (7) is replaced by

$$M^e = \sum_{j=1}^{4} \hat{V}_j^e \hat{M}_j^e \tag{29}$$

where

$$\left.\begin{aligned} \hat{M}_1^e &= J_p(ka)\, M_1^e \\ \hat{M}_j^e &= M_j^e + C_j^e M_1^e, \quad j=2,3,4 \end{aligned}\right\} \tag{30}$$

$$C_j^e = - S_{jp}^e / S_{1p}^e \tag{31}$$

As a result, (23) is replaced by

$$\frac{1}{2}\hat{V}_1^e\left(\frac{S_{1p}^e\cos(p\phi)}{H_p^{(2)}(ka)}+J_p(ka)\sum_{\substack{n=0\\n\neq p}}^{\infty}\frac{S_{1n}^e\cos(n\phi)}{J_n(ka)\,H_n^{(2)}(ka)}\right)$$

$$+\frac{1}{2}\sum_{j=2}^{4}\hat{V}_j^e\left(\sum_{\substack{n=0\\n\neq p}}^{\infty}\frac{(S_{jn}^e+C_j^eS_{1n}^e)\cos(n\phi)}{J_n(ka)\,H_n^{(2)}(ka)}\right)$$

$$=\sum_{n=0}^{\infty}\frac{\varepsilon_n j^n\cos(n\alpha)\cos(n\phi)}{2H_n^{(2)}(ka)},\quad |\phi|\leq\phi_o \tag{32}$$

Numerical solution of (32) should not be difficult when $|J_p(ka)|$ is very small because, in contrast to (23), (32) does not contain any huge cos $(p\phi)$ terms which could obscure all the other terms.

If $|J_o(ka)|$ is very small, (26) is retained. However, if $|J_p(ka)|$ is very small where p is a positive integer, then (24) is replaced by

$$M^o=\sum_{j=1}^{4}\hat{V}_j^o\,\hat{M}_j^o \tag{33}$$

where

$$\left.\begin{aligned}\hat{M}_1^o&=J_p(ka)\,M_1^o\\ \hat{M}_j^o&=M_j^o+C_j^o\,M_1^o,\quad j=2,3,4\end{aligned}\right\} \tag{34}$$

$$C_j^o=-S_{jp}^o/S_{1p}^o \tag{35}$$

so that (26) is replaced by

$$\frac{1}{2}\hat{V}_1^o\left(\frac{S_{1p}^o \sin(p\phi)}{H_p^{(2)}(ka)} + J_p(ka)\sum_{\substack{n=1\\ n\neq p}}^{\infty}\frac{S_{1n}^o \sin(n\phi)}{J_n(ka)\,H_n^{(2)}(ka)}\right)$$

$$+\frac{1}{2}\sum_{j=2}^{4}\hat{V}_j^o\left(\sum_{\substack{n=1\\ n\neq p}}^{\infty}\frac{(S_{jn}^o + C_j^o S_{1n}^o)\sin(n\phi)}{J_n(ka)\,H_n^{(2)}(ka)}\right)$$

$$=\sum_{n=1}^{\infty}\frac{j^n \sin(n\alpha)\sin(n\phi)}{H_n^{(2)}(ka)}, \quad |\phi|\leq\phi_o \tag{36}$$

Equation (36) is valid for $p \geq 1$. If $p = 0$, we revert to (26). Numerical solution of (36) should not be difficult when $|J_p(ka)|$ is very small because, in contrast to (26), (36) does not contain any huge sin $(p\phi)$ terms which could obscure all the other terms.

Equations (5) and (6) can be viewed as operator equations. For example, (5) is

$$L\,M^e = g \tag{37}$$

where L is an operator and g is a known function. Since (19) is $L\,M_j^e$ where M_j^e is given by (12), it is evident that

$$L\cos(p\phi) = \frac{2\cos(p\phi)}{\pi\eta ka\,J_p(ka)\,H_p^{(2)}(ka)} \tag{38}$$

Hence, when $|J_p(ka)|$ is very small, the eigenvalue associated with the eigenfunction cos $(p\phi)$ is very large in magnitude. In this case, the expansion functions $\{M_j^e,\ j=1,2,3,4\}$ are not good because each one of them contains cos $(p\phi)$ so that all of the functions $\{L\,M_j^e,\ j=1,2,3,4\}$, being

roughly proportional to cos (pφ), are nearly indistinguishable from each other. The expansion functions $\{\hat{M}_j^e,\ j=1,2,3,4\}$ are better because $\hat{M}_1^e$, which contains cos (pφ), is normalized so that $L\,\hat{M}_1^e$ remains finite, and none of the functions $\{\hat{M}_j^e,\ j=2,3,4\}$ contains cos (pφ). Therefore, none of the functions $\{L\,\hat{M}_j^e,\ j=2,3,4\}$ contains cos (pφ). Since none of them are dominated by cos (pφ), the functions $\{L\,\hat{M}_j^e,\ j=2,3,4\}$ are easily distinguishable from each other and from $L\,\hat{M}_1^e$.

IV. TESTING FUNCTIONS

In this Section, 4 linear equations are extracted from the functional equation (32) by multiplying (32) by each of 4 even functions called testing functions and integrating from $-\phi_o$ to ϕ_o with respect to φ. Similarly, 4 linear equations are extracted from (36) by multiplying (36) by each of 4 odd testing functions and integrating over the slot.

Called $\{W_i^e,\ i=1,2,3,4\}$, the even testing functions are defined by

$$W_i^e = (\phi/\phi_o)^{2i-2}, \quad i=1,2,3,4 \tag{39}$$

Multiplying (32) by W_i^e and integrating over the slot, we obtain 4 equations, one for each value of i. In matrix notation, these equations are

$$Y^e \vec{\hat{V}}^e = \vec{I}^e \tag{40}$$

where $\vec{\hat{V}}^e$ is the column vector whose jth element is $\hat{V}_j^e$ and Y^e is the 4×4 matrix whose elements are given by

$$Y^e_{i1} = \frac{F^e_{ip}\, S^e_{1p}}{H^{(2)}_p(ka)} + J_p(ka) \sum_{\substack{n=0 \\ n\neq p}}^{\infty} \frac{F^e_{in}\, S^e_{1n}}{J_n(ka)\, H^{(2)}_n(ka)}, \quad i=1,2,3,4 \tag{41}$$

$$Y^e_{ij} = \sum_{\substack{n=0 \\ n\neq p}}^{\infty} \frac{F^e_{in}(S^e_{jn} + C^e_j\, S^e_{1n})}{J_n(ka)\, H^{(2)}_n(ka)}, \quad \begin{cases} i = 1,2,3,4 \\ j = 2,3,4 \end{cases} \tag{42}$$

The coefficient F^e_{in} arises when the normalized magnetic field on the left-hand side of (32) is multiplied by W^e_i and integrated over the slot:

$$F^e_{in} = \frac{1}{2} \int_{-\phi_o}^{\phi_o} (\phi/\phi_o)^{2i-2} \cos(n\phi)\, d\phi \tag{43}$$

The coefficient F^e_{in} is evaluated in Appendix B. In (40), $\vec{I}^e$ is the column vector whose elements are given by

$$I^e_i = 2 \sum_{n=0}^{\infty} \frac{\varepsilon_n j^n F^e_{in} \cos(n\alpha)}{2\, H^{(2)}_n(ka)}, \quad i = 1,2,3,4 \tag{44}$$

The odd testing functions are defined by

$$W^o_i = (\phi/\phi_o)^{2i-1}, \quad i = 1,2,3,4 \tag{45}$$

We multiply (36) by W^o_i and integrate over the slot. Doing this for $i = 1,2,3$, and 4, we obtain the matrix equation

$$Y^o \vec{V}^o = \vec{I}^o \tag{46}$$

where $\vec{V}^o$ is the column vector whose jth element is $\hat{V}^o_j$, and Y^o is the 4×4 matrix whose elements are given by

$$Y^o_{i1} = \frac{F^o_{ip}\, S^o_{1p}}{H^{(2)}_p(ka)} + J_p(ka) \sum_{\substack{n=1 \\ n\neq p}}^{\infty} \frac{F^o_{in}\, S^o_{1n}}{J_n(ka)\, H^{(2)}_n(ka)}, \quad i=1,2,3,4 \tag{47}$$

$$Y^o_{ij} = \sum_{\substack{n=1 \\ n\neq p}}^{\infty} \frac{F^o_{in}\,(S^o_{jn} + C^o_j\, S^o_{1n})}{J_n(ka)\, H^{(2)}_n(ka)}\,, \quad \begin{cases} i=1,2,3,4 \\ j=2,3,4 \end{cases} \tag{48}$$

where

$$F^o_{in} = \frac{1}{2} \int_{-\phi_o}^{\phi_o} (\phi/\phi_o)^{2i-1} \sin(n\phi)\, d\phi \tag{49}$$

The coefficient F^o_{in} is evaluated in Appendix B. In (46), $\vec{I}^o$ is the column vector whose elements are given by

$$I^o_i = 2 \sum_{n=1}^{\infty} \frac{j^n\, F^o_{in} \sin(n\alpha)}{H^{(2)}_n(ka)}\,, \quad i = 1,2,3,4 \tag{50}$$

Actually, (46)-(48) are valid only for $p > 0$. For $p = 0$, we multiply (26) by W^o_i and integrate over the slot. Doing this for i=1,2,3, and 4, we obtain (46) with the elements of $\vec{\hat{V}}^o$ given by

$$\hat{V}^o_j = V^o_j, \tag{51}$$

with the elements of Y^o given by

$$Y^o_{ij} = \sum_{n=1}^{\infty} \frac{F^o_{in}\, S^o_{jn}}{J_n(ka)\, H^{(2)}_n(ka)}\,, \tag{52}$$

and with the elements of $\vec{I}^o$ given by (50).

Solving (40) for $\vec{\hat{V}}^e$, we obtain $\hat{V}^e_j$. Now, M^e is given by (29). In view of (30), M^e is also given by (7) with

$$\left.\begin{aligned} V^e_1 &= J_p(ka)\, \hat{V}^e_1 + \sum_{i=2}^{4} C^e_i\, \hat{V}^e_i \\ V^e_j &= \hat{V}^e_j\,, \quad j = 2,3,4 \end{aligned}\right\} \tag{53}$$

Solving (46) for $\vec{\hat{V}}^o$, we obtain $\hat{V}^o_j$. Now, M^o is given by (33). In view of (34), M^o is also given by (24) with

$$\left.\begin{aligned} V^o_1 &= J_p(ka)\, \hat{V}^o_1 + \sum_{i=2}^{4} C^o_i\, \hat{V}^o_i \\ V^o_j &= \hat{V}^o_j,\ j = 2,3,4 \end{aligned}\right\} \tag{54}$$

Actually, (54) is valid only for $p > 0$. For $p = 0$, M^o is given by (24) with V_j^o of (51):

$$V_j^o = \hat{V}_j^o \ , \quad j = 1,2,3,4 \tag{55}$$

Finally, $\underline{M}$ is given by (4) where M^e is given by (7) with V_j^e of (53), and M^o is given by (24) with V_j^o of (54) and (55):

$$\underline{M} = \underline{u}_\phi \sum_{j=1}^{4} (V_j^e M_j^e + V_j^o M_j^o) \tag{56}$$

The electric field in Fig. 2 is $\underline{u}_z E_z$ where

$$E_z = \begin{cases} E_z^{sc} + E_z^a(\underline{M}) & , \ \rho \geq a \\ E_z^b(-\underline{M}) & , \ \rho \leq a \end{cases} \tag{57}$$

where E_z^{sc}, $E_z^a(\underline{M})$, and $E_z^b(-\underline{M})$ are the z components of the electric fields due to the incident wave, $\underline{M}$, and $-\underline{M}$, respectively. From (1) and [13, eq. (5-107)], we obtain

$$E_z^{sc} = \sum_{n=0}^{\infty} \varepsilon_n j^n \left[J_n(k\rho) - \frac{J_n(ka)}{H_n^{(2)}(ka)} H_n^{(2)}(k\rho)\right] \cos(n(\phi-\alpha)) \tag{58}$$

From (56), we have

$$\left.\begin{aligned} E_z^a(\underline{M}) &= \sum_{j=1}^{4} (V_j^e E_z^a(\underline{u}_\phi M_j^e) + V_j^o E_z^a(\underline{u}_\phi M_j^o)) \\ E_z^b(-\underline{M}) &= \sum_{j=1}^{4} (V_j^e E_z^b(-\underline{u}_\phi M_j^e) + V_j^o E_z^b(-\underline{u}_\phi M_j^o)) \end{aligned}\right\} \tag{59}$$

Now, $E_z^a(\underline{u}_\phi M_j^e)$ is E_z^a of (11) and $E_z^b(-\underline{u}_\phi M_j^e)$ is E_z^b of (11). Similarly,

$$\left.\begin{aligned} E_z^a(\underline{u}_\phi M_j^o) &= \sum_{n=1}^{\infty} \frac{S_{jn}^o H_n^{(2)}(k\rho) \sin(n\phi)}{H_n^{(2)}(ka)} \\ E_z^b(-\underline{u}_\phi M_j^o) &= \sum_{n=1}^{\infty} \frac{S_{jn}^o J_n(k\rho) \sin(n\phi)}{J_n(ka)} \end{aligned}\right\} \tag{60}$$

so that (59) expands to

$$E_z^a(\underline{M}) = \sum_{n=0}^{\infty} \frac{B_n^e H_n^{(2)}(k\rho) \cos(n\phi)}{H_n^{(2)}(ka)} + \sum_{n=1}^{\infty} \frac{B_n^o H_n^{(2)}(k\rho) \sin(n\phi)}{H_n^{(2)}(ka)} \tag{61}$$

$$E_z^b(-\underline{M}) = \sum_{n=0}^{\infty} \frac{B_n^e J_n(k\rho) \cos(n\phi)}{J_n(ka)} + \sum_{n=1}^{\infty} \frac{B_n^o J_n(k\rho) \sin(n\phi)}{J_n(ka)} \tag{62}$$

where

$$B_n^e = \sum_{j=1}^{4} V_j^e S_{jn}^e \tag{63}$$

$$B_n^o = \sum_{j=1}^{4} V_j^o S_{jn}^o \tag{64}$$

In view of (31), substitution of (53) into (63) gives

$$B_p^e = J_p(ka) \hat{V}_1^e S_{1p}^e \tag{65}$$

Substituting (54) into (64) and using (35), we obtain

$$B_p^o = J_p(ka) \hat{V}_1^o S_{1p}^o \quad , \quad p \neq 0 \tag{66}$$

From (65) and (66), it is evident that (62) remains finite as $J_p(ka)$ approaches zero. When $\rho = 0$, (62) reduces to

$$E_z^b(-\underline{M}) = \frac{B_o^e}{J_o(ka)} \tag{67}$$

Since B_o^e is given by (65) when $p = 0$ and by (63) when $p \neq 0$, (67) becomes

$$E_z^b(-\underline{M}) = \left\{ \begin{array}{ll} \hat{V}_1^e S_{10}^e & , \ p = 0 \\ \dfrac{1}{J_o(ka)} \displaystyle\sum_{j=1}^{4} V_j^e S_{jo}^e & , \ p \neq 0 \end{array} \right\} , \quad \rho = 0 \tag{68}$$

In the preceding paragraph, we found $\underline{u}_z E_z$, the electric field in Fig. 2. Called $\underline{H}$, the magnetic field in Fig. 2 is given by

$$\underline{H} = \frac{j}{k\eta} (\nabla E_z \times \underline{u}_z) \tag{69}$$

Since $\underline{M}$ was determined such that the situation in Fig. 2 is equivalent to that in Fig. 1, the fields in Fig. 2 are the same as those in Fig. 1. Thus, we have attained our objective, which was to find the fields everywhere in Fig. 1.

V. INTERIOR FIELD AT RESONANCE

If ka is such that the cavity is resonant, that is, if there is a non-negative integer p such that $J_p(ka) = 0$, then an approximate expression for the z component E_z of electric field inside the cylinder can be found in the following manner. This approximate expression serves to check values of the interior field calculated by means of (62) and (68).

If there was no aperture, the magnetic field immediately outside the cylinder due to the incident electric field (1) would be the short-circuit magnetic field whose ϕ component $[H_\phi^{sc}]_{\rho=a}$ is given by (21). In this case, an electric current $\underline{J}$ given by

$$\underline{J} = \underline{u}_z \left\{ [H_\phi^{sc}]_{\rho=a} + A_p^e \cos(p\phi) + A_p^o \sin(p\phi) \right\} \tag{70}$$

is induced on the cylinder. In (70), A_p^e and A_p^o are arbitrary constants. If $p = 0$, then A_p^o drops out. The part of $\underline{J}$ associated with A_p^e and A_p^o radiates only inside the cylinder where its E_z is given by

$$E_z = - \frac{j\eta J_p(k\rho)}{J_p'(ka)} [A_p^e \cos(p\phi) + A_p^o \sin(p\phi)] \tag{71}$$

Since the electric current $\underline{u}_z[H_\phi^{sc}]_{\rho=a}$ produces a field which cancels the incident field inside the cylinder, E_z of (71) is the total electric field inside the cylinder.

If A_p^e and A_p^o are determined such that both $\underline{J}$ and $\frac{\partial \underline{J}}{\partial \phi}$ vanish at $\phi = 0$, then $\underline{J}$ will be the approximate electric current that would exist if there was a narrow aperture at $\phi = 0$. If $p = 0$, we can only require that $\underline{J}$ vanish at $\phi = 0$. Substituting (21) into (70) and forcing $\underline{J}$ and $\frac{\partial J}{\partial \phi}$ to vanish at $\phi = 0$, we obtain

$$A_p^e = - \frac{4}{\pi\eta ka} \sum_{n=0}^{\infty} \frac{\varepsilon_n j^n \cos(n\alpha)}{2H_n^{(2)}(ka)} \tag{72}$$

$$A_p^o = - \frac{4}{p\pi\eta ka} \sum_{n=1}^{\infty} \frac{n j^n \sin(n\alpha)}{H_n^{(2)}(ka)}, \quad p \neq 0 \tag{73}$$

Substitution of (72) and (73) into (71) gives

$$E_z = \frac{4j J_p(k\rho)}{\pi ka J_p'(ka)} \left[\left(\sum_{n=0}^{\infty} \frac{\varepsilon_n j^n \cos(n\alpha)}{2H_n^{(2)}(ka)} \right) \cos(p\phi) + \frac{1}{p} \left(\sum_{n=1}^{\infty} \frac{n j^n \sin(n\alpha)}{H_n^{(2)}(ka)} \right) \sin(p\phi) \right] \tag{74}$$

where the $\frac{1}{p}$ term is to be discarded if $p = 0$. Thanks to the Wronskian [13, Eq. (D-17)] and the fact that $J_p(ka) = 0$, (74) becomes

$$E_z = 2J_p(k\rho) H_p^{(2)}(ka) \left[\left(\sum_{n=0}^{\infty} \frac{\varepsilon_n j^n \cos(n\alpha)}{2H_n^{(2)}(ka)} \right) \cos(p\phi) + \frac{1}{p} \left(\sum_{n=1}^{\infty} \frac{n j^n \sin(n\alpha)}{H_n^{(2)}(ka)} \right) \sin(p\phi) \right] \tag{75}$$

where the $\frac{1}{p}$ term is to be discarded if $p = 0$. When $p = 0$ and $\rho = 0$,

E_z of (75) reduces to the $\psi(0)$ in [14, last line of p. 1391] with $A = 1$, α replaced by $\alpha - \pi$, and $-i$ replaced by j. As given by (75), E_z is the field inside the cylinder when the aperture is narrow and when p is a non-negative integer such that $J_p(ka) = 0$. Since this E_z does not depend on the width of the aperture, we deduce that the amount of TM field that enters a resonant circular cylindrical cavity through an infinitely long but narrow slot does not depend on the width of the slot.

VI. NUMERICAL RESULTS AND DISCUSSION

By means of a computer program that will be described and listed in a forthcoming report, $|E_z|$ of (57) was calculated in the aperture and at the center of the cylinder. This program was also designed to calculate $|E_z|$ at equally spaced points along the line that extends from the center of the cylinder to the center of the aperture. All values of $|E_z|$ presented in this report were obtained by truncating the summations in (41) and (42) at $n = 10{,}000$. Unless otherwise stated the 4×4 matrix Y^e with elements (41) and (42) was used.

Figures 4 and 5 show the field amplitude $|E_z|$ in the aperture for $\phi_o = 10°$, $\alpha = 0$, and various values of ka. Figures 6 and 7 show $|E_z|$ in the aperture for $\phi_o = 30°$, $\alpha = 0$, and the same values of ka. The curves in Figs. 6 and 7 agree reasonably well with those in [1, Fig. 2] and [2, Figs. 8 and 9]. However, the curves in Figs. 4 and 5 are noticeably different from those in [2, Figs. 6 and 7]. We believe that our aperture field amplitudes for $\phi_o = 10°$ are more accurate than those in [2]. Furthermore, we conjecture that the method used in [1] and [2], the E-field integral equation method, will give worse results

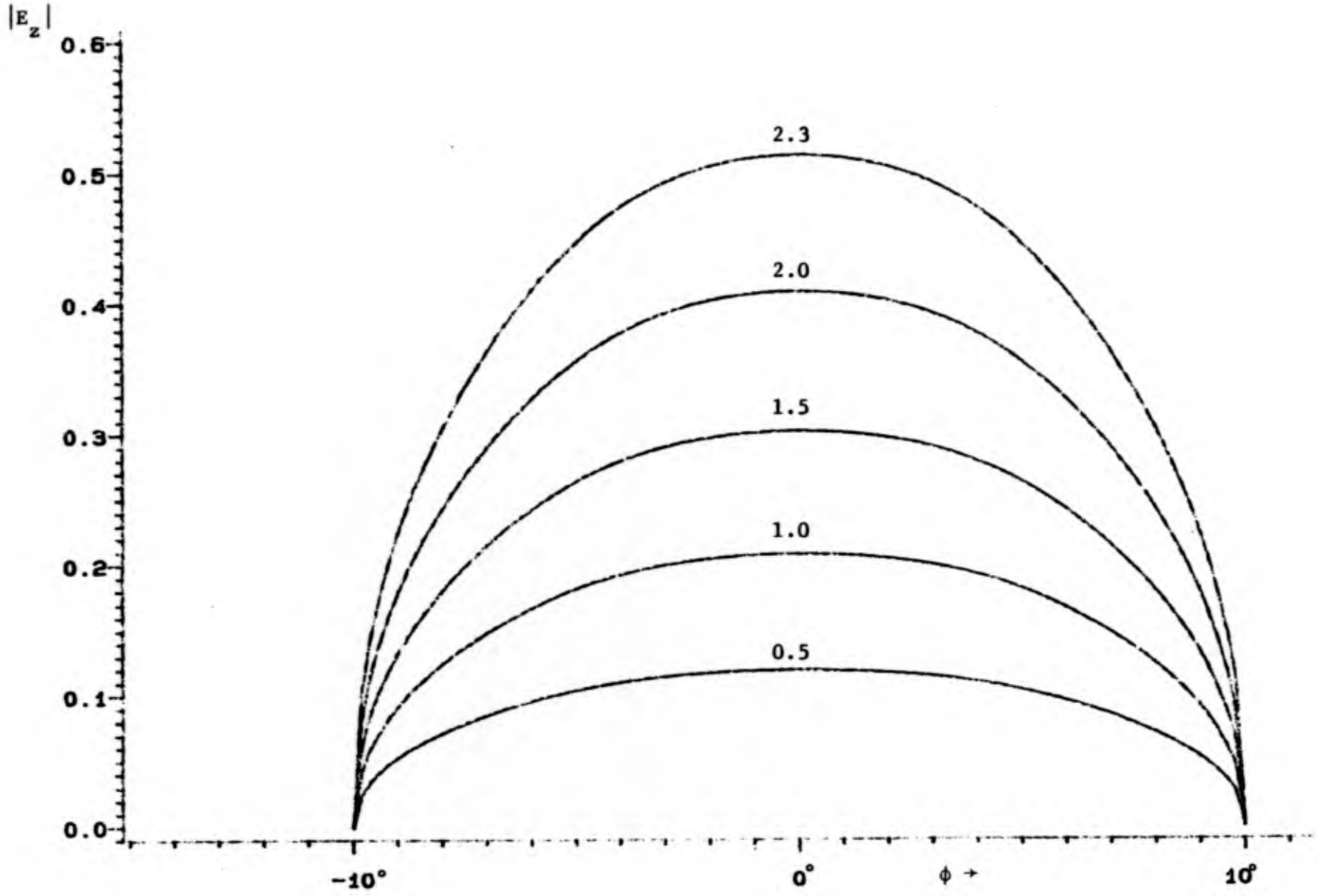

Fig. 4. Field amplitude $|E_z|$ in the aperture for $\phi_o = 10°$, $\alpha = 0°$, and various values of ka.

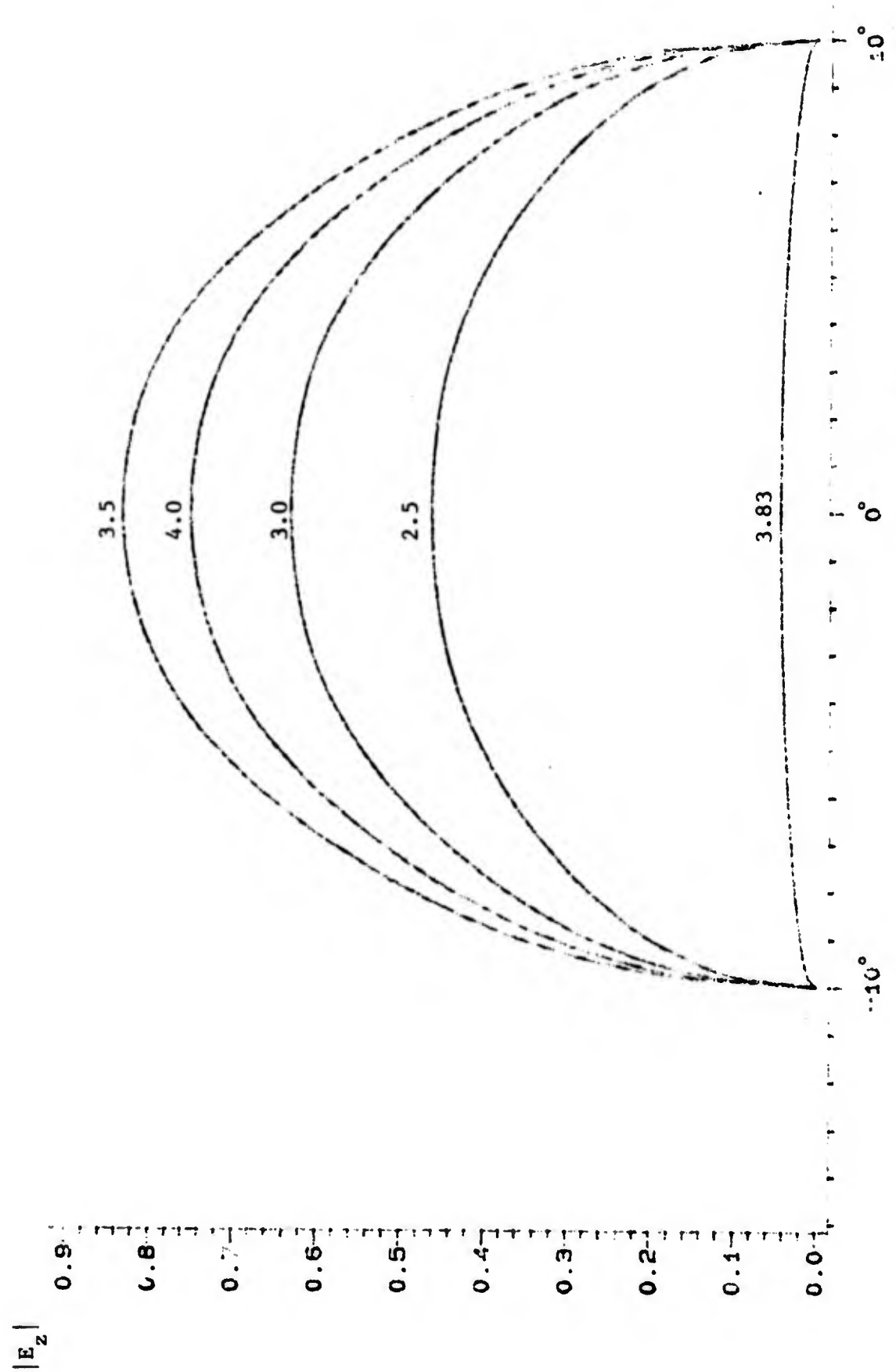

Fig. 5. Field amplitude $|E_z|$ in the aperture for $\phi_o = 10°$, $\alpha = 0°$, and various values of ka.

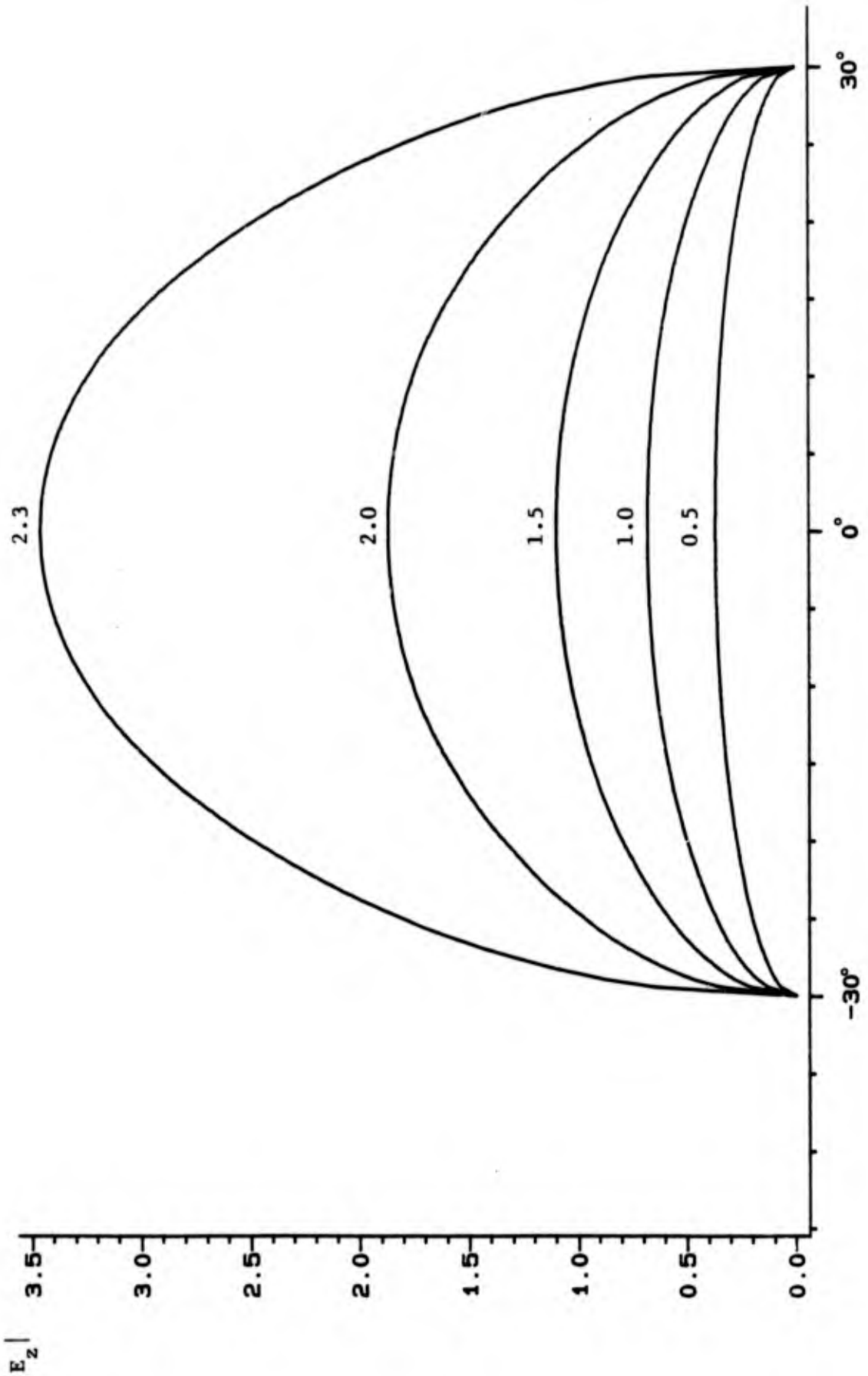

Fig. 6. Field amplitude $|E_z|$ in the aperture for $\phi_o = 30°$, $\alpha = 0°$, and various values of ka.

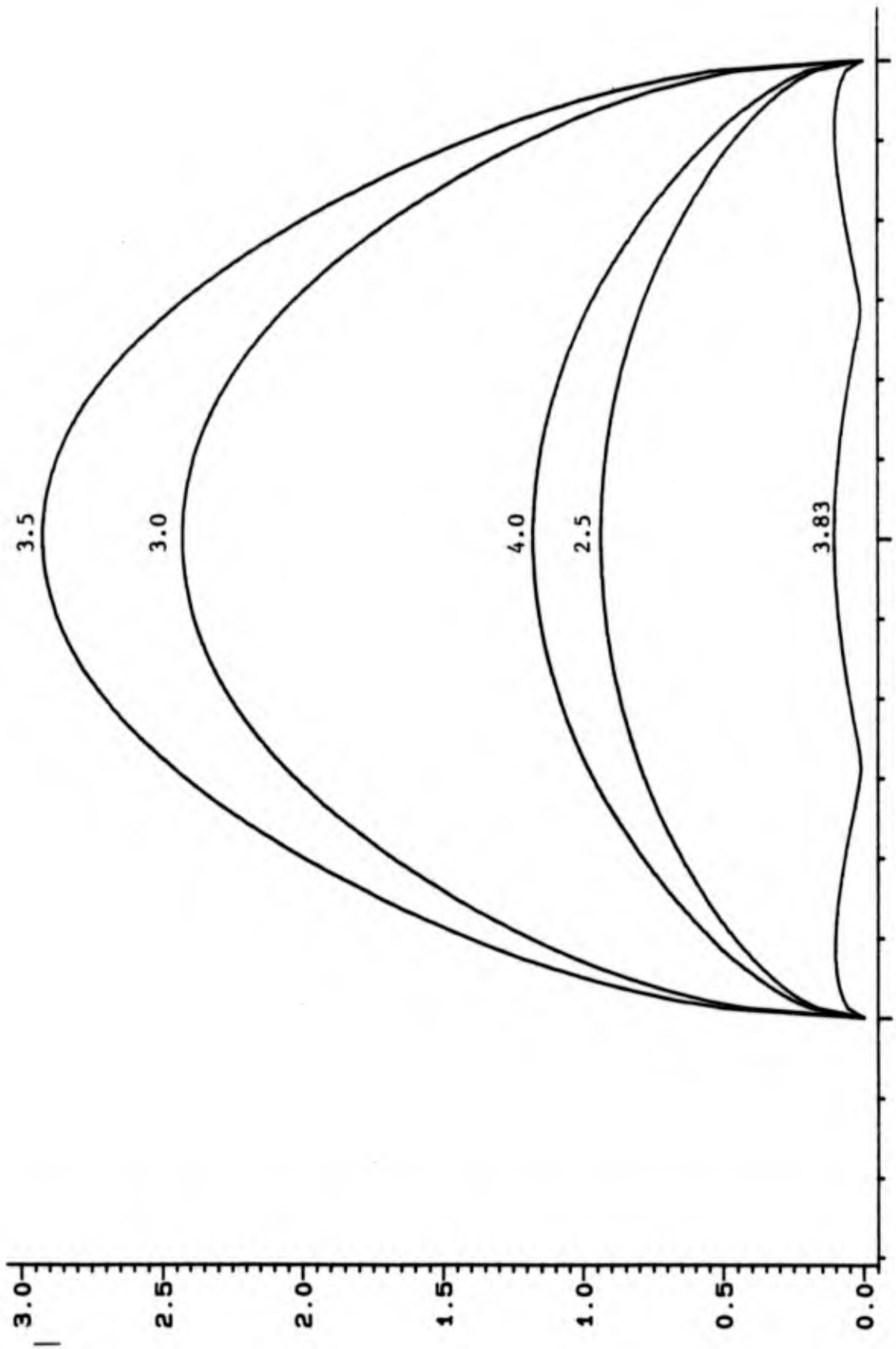

Fig. 7. Field amplitude $|E_z|$ in the aperture for $\phi_o = 30°$, $\alpha = 0°$, and various values of ka.

for apertures for which ϕ_o is less than 10°.

Figures 8 to 11 show $|E_z|$ in the aperture for $\alpha = 0$ and 4 different combinations of ϕ_o and ka. The values of $|E_z|$ in these figures should be slightly different from those in [15, Figs. 23, 16, 17, and 25] because the aperture of [15] is the plane strip connecting the edges of the conductor whereas our aperture is the arc whose equation is ($\rho = a$, $-\phi_o \leq \phi \leq \phi_o$). Calculated values of $|E_z|$ at the center of the plane strip and at the center of the arc are presented in Table 1.

Table 1. Field amplitudes at ($\rho = a \cos \phi_o$, $\phi = 0$) and at ($\rho = a, \phi = 0$).

ϕ_o	ka	$\lvert E_z \rvert$ at $\rho = a \cos \phi_o$	$\lvert E_z \rvert$ at $\rho = a$
1.25°	2	0.0461	0.0466
5°	1	0.0985	0.1027
5°	$\pi/2$	0.1466	0.1528
10°	1	0.1919	0.2087
15°	1	0.2815	0.3190
15°	3	0.9691	1.0672
30°	1	0.5351	0.6797

Figure 12 shows $|E_z|$ at the center of the aperture versus ka for $\alpha=0$ and ϕ_o = 10° and 30°. The solid curve is for ϕ_o = 10°, and the asterisks represent crude values of $|E_z|$ for ϕ_o = 10°. Crude values of $|E_z|$ are those obtained by retaining only the first equation and the first unknown in (40), that is, Y^e, $\vec{V}^e$, and $\vec{I}^e$ are replaced by Y^e_{11}, $\hat{V}^e_1$, and I^e_1, respectively. The dashed curve is for ϕ_o = 30°,

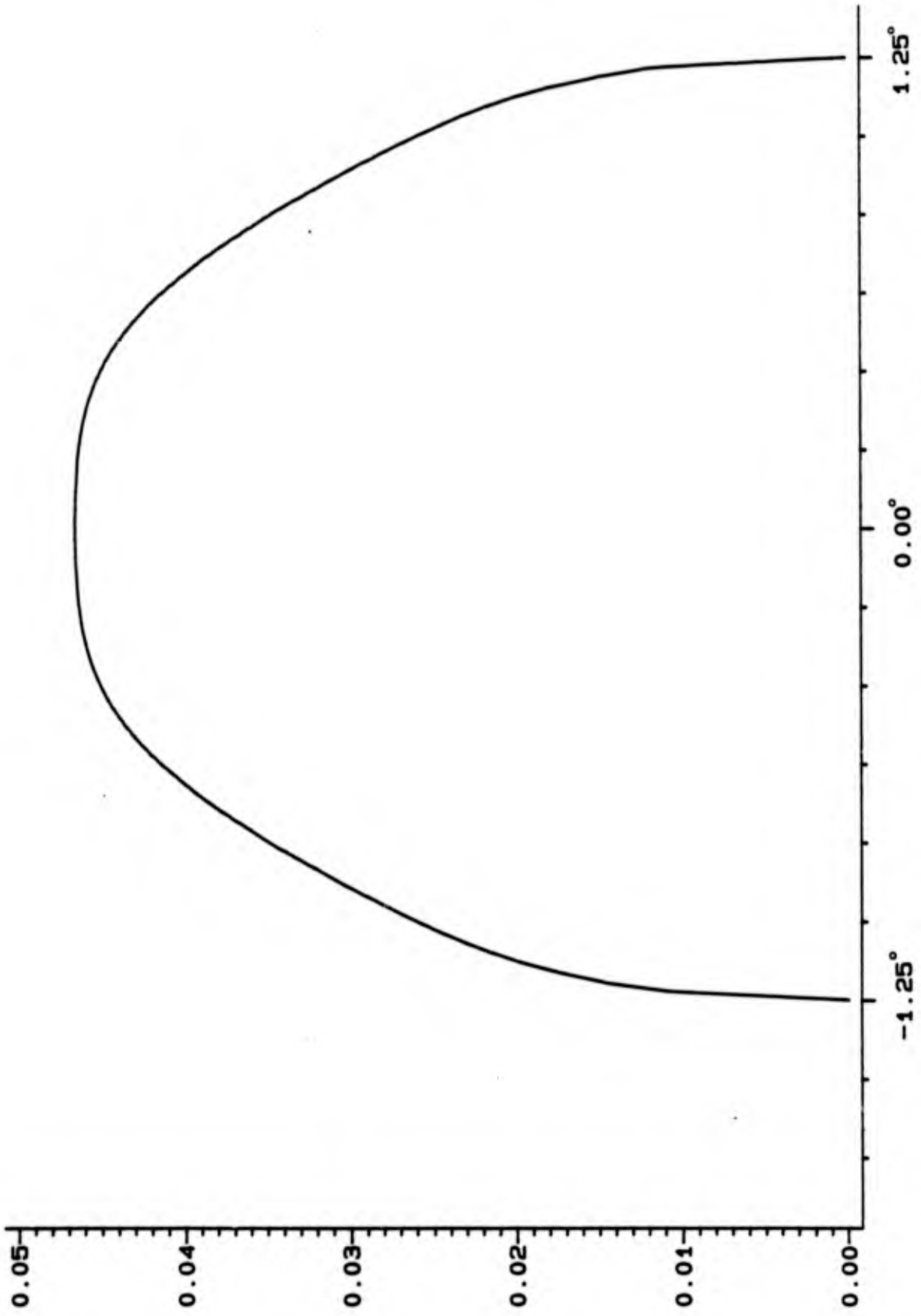

Fig. 8. Field amplitude $|E_z|$ in the aperture for $\phi_o = 1.25°$, $\alpha = 0°$, and ka = 2.

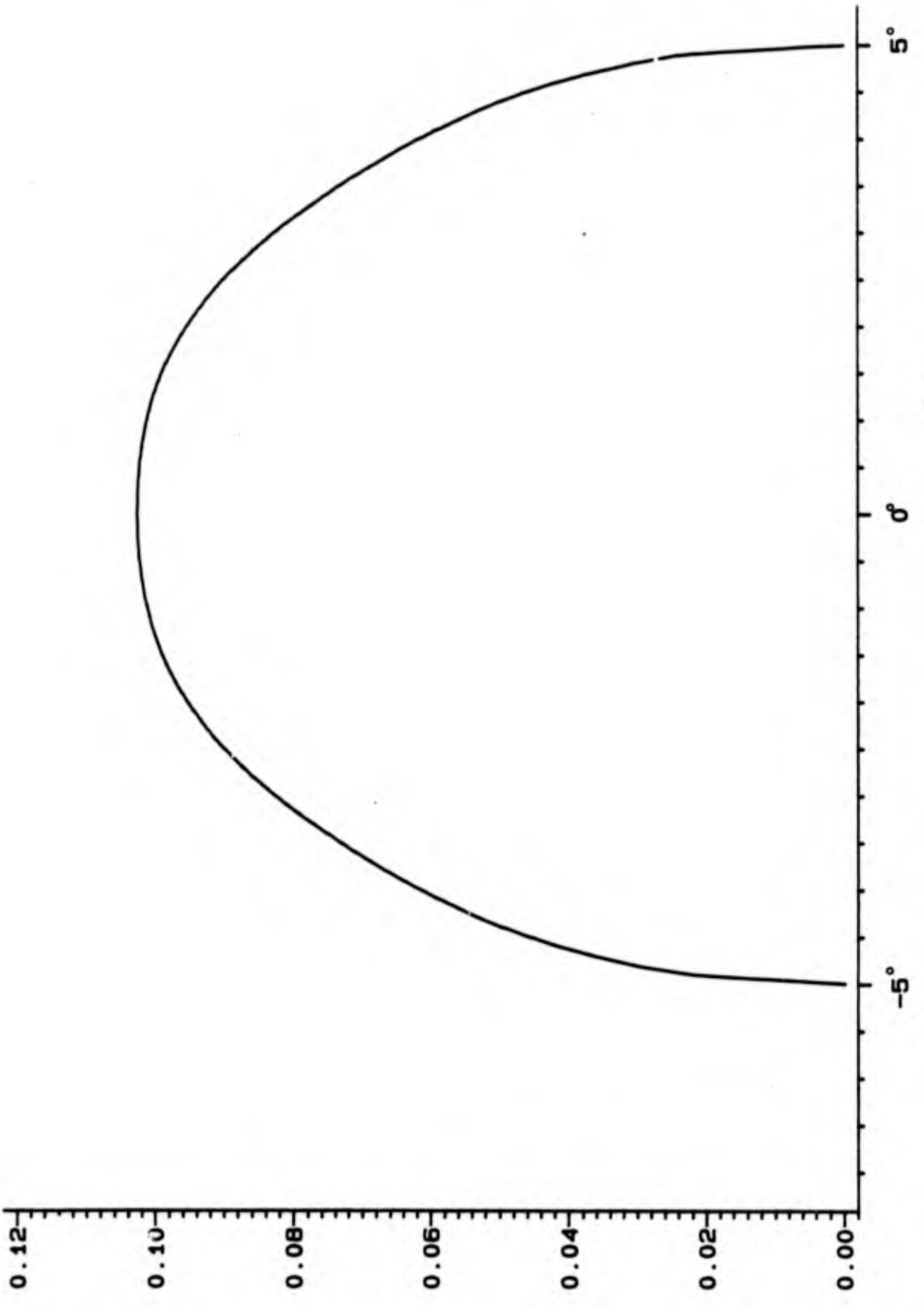

Fig. 9. Field amplitude $|E_z|$ in the aperture for $\phi_o = 5°$, $\alpha = 0°$, and ka = 1.

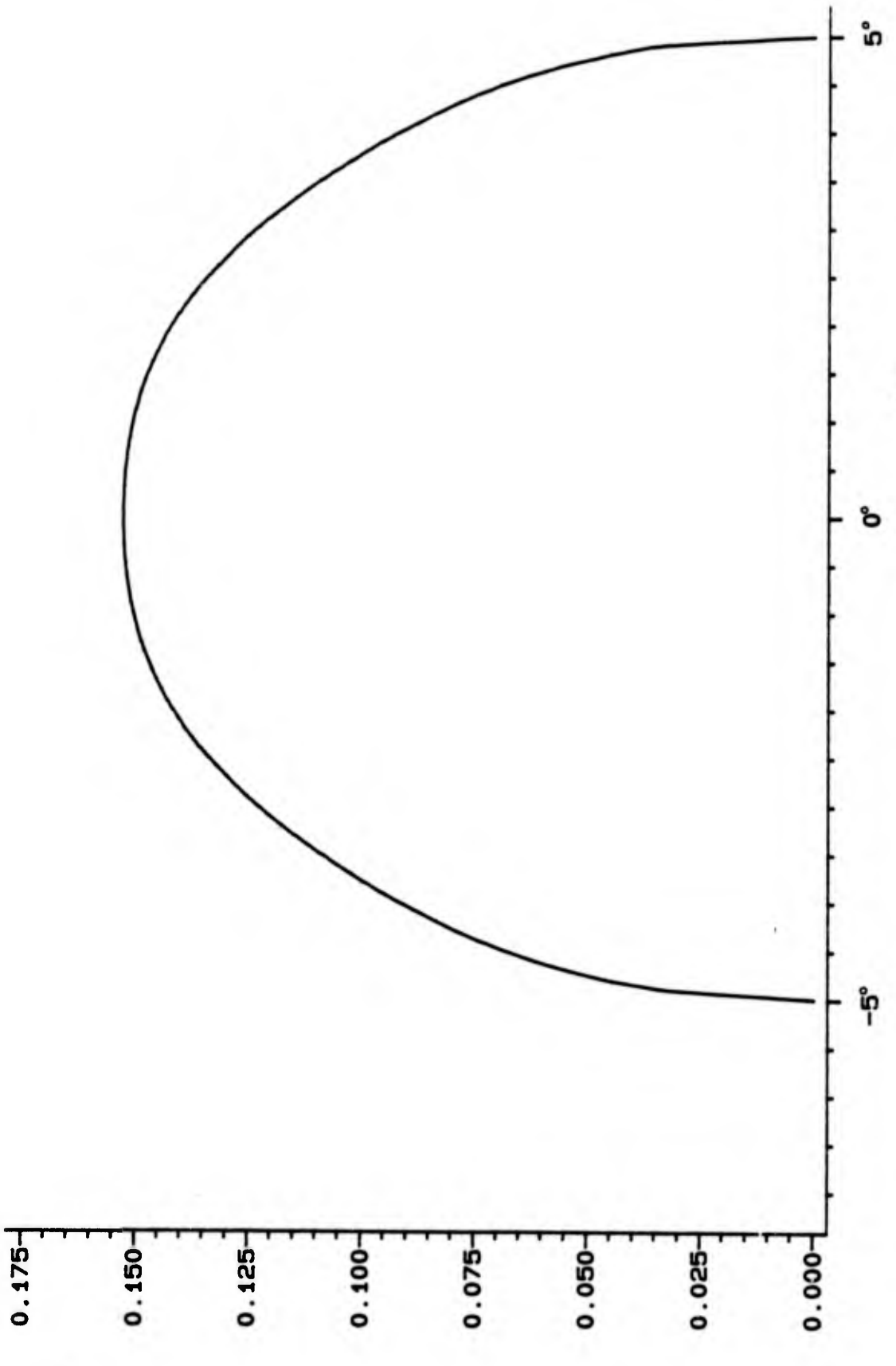

Fig. 10. Field amplitude $|E_z|$ in the aperture for $\phi_o = 5°$, $\alpha = 0°$, and $ka = \pi/2$.

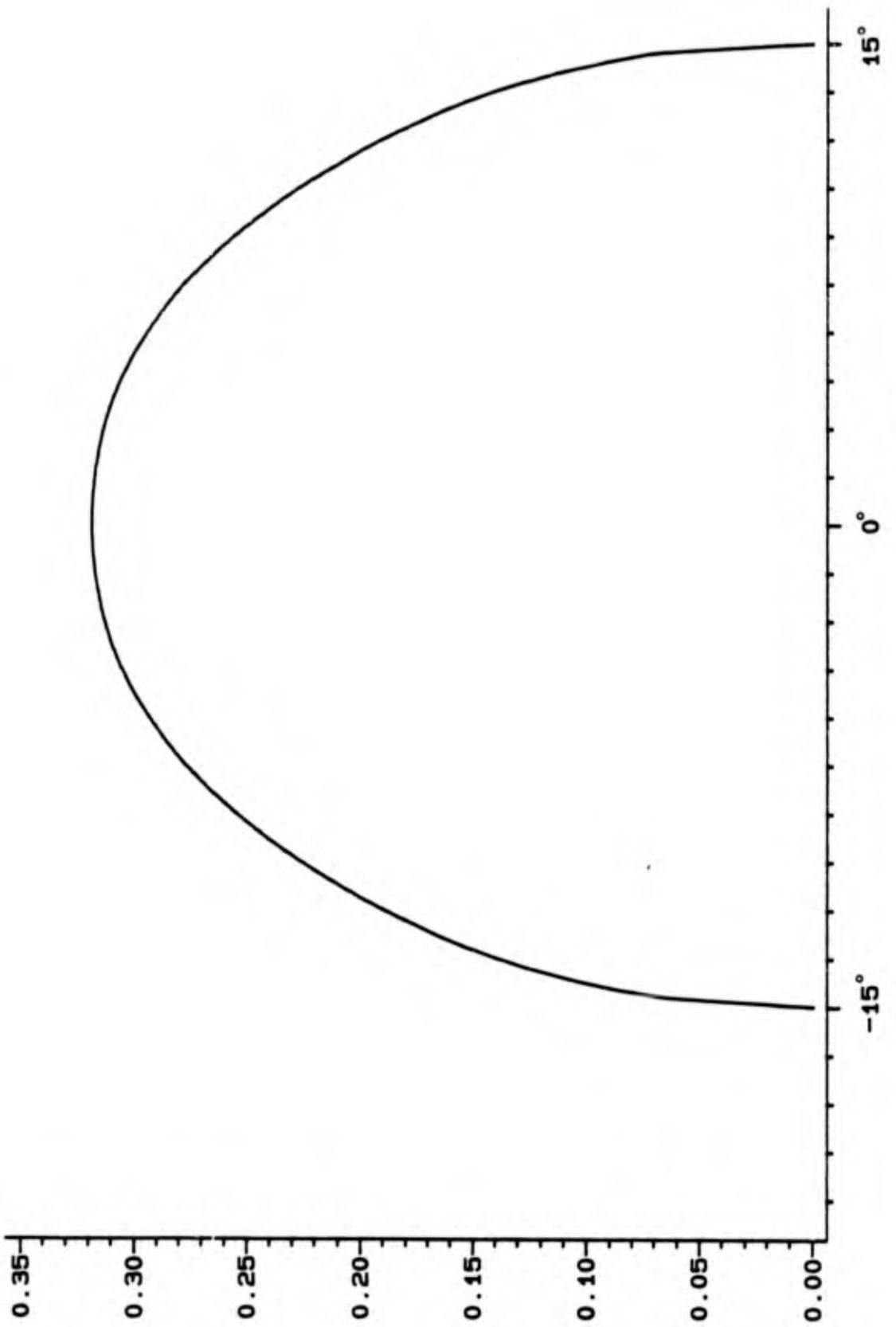

Fig. 11. Field amplitude $|E_z|$ in the aperture for $\phi_o = 15°$, $\alpha = 0°$, and ka = 1.

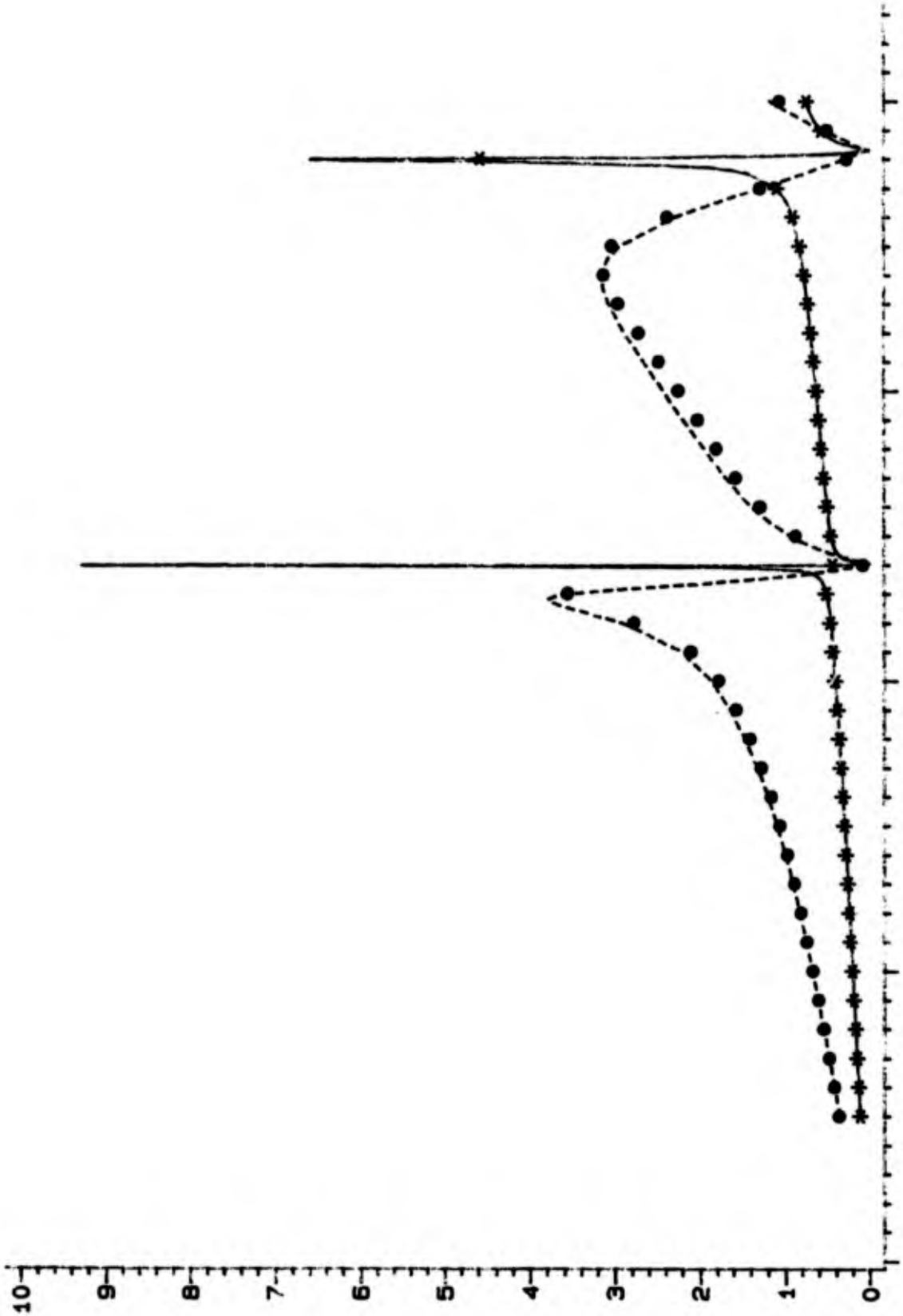

Fig. 12. Field amplitude $|E_z|$ at the center of the aperture versus ka for $\alpha = 0°$. The solid curve is for $\phi_o = 10°$. The dashed curve is for $\phi_o = 30°$.

and the large dots represent crude values of $|E_z|$ for $\phi_o = 30°$. In Fig. 13, the data of Fig. 12 are plotted on a logarithmic scale. Since the crude values of $|E_z|$ lie so close to the dashed and solid curves in Figs. 12 and 13, our matrix solution for $|E_z|$ appears to have converged. We do not think that $|E_z|$ would change much if more expansion functions were used. Our plot of $|E_z|$ for $\phi_o = 30°$ agrees with that in [1, Fig. 3]. However, our $|E_z|$ for $\phi_o = 10°$ has a much sharper peak in the vicinity of ka = 2.4. Furthermore, in contrast to that in [1, Fig. 3], our $|E_z|$ for $\phi_o = 10°$ also has a sharp peak in the vicinity of ka = 3.8 and no broad minimum near ka = 1.

The crude values of $|E_z|$ in Figs. 12 and 13 were obtained by using the single expansion function M_1^e of (8) and the single testing function W_1^e of (39). For $\phi_o = 5°$, $\alpha = 0°$, and ka = $\pi/2$, the crude value of $|E_z|$ at the center of the aperture is 0.1563. This compares with 0.1528 in Table 1 and 0.1534 in [3, Table 1] calculated by means of the Fourier series method of solution described in [3]. This Fourier series method of solution employs the single expansion function $\sqrt{1-(\phi/\phi_o)^2}$ and the single testing function $\sqrt{1-(\phi/\phi_o)^2}$. In the method presented in [14, pp. 1387-1392], the single expansion function $\sqrt{1-(\phi/\phi_o)^2}$ is used and (2) is enforced at the center of the aperture. This enforcement is equivalent to having a testing function which is a Dirac delta function at the center of the aperture. The method of calculation of the crude $|E_z|$, the Fourier series method of [3], and the method presented in [14] differ only in that they employ different testing functions.

Figure 14 shows $|E_z|$ at the center of the cylinder versus ka for $\alpha = 0°$. The solid curve is for $\phi_o = 10°$, and the asterisks represent crude values

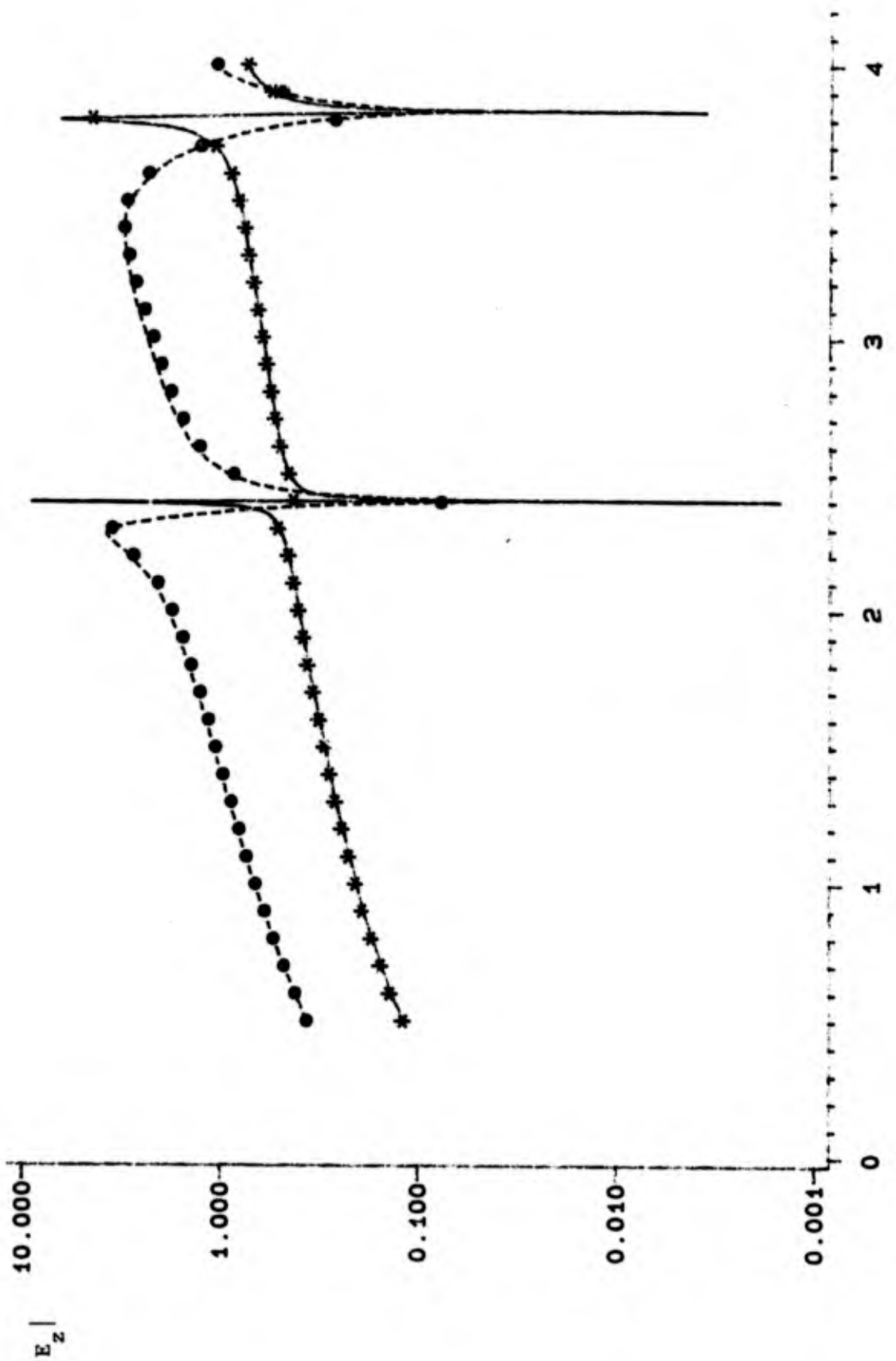

Fig. 13. Field amplitude $|E_z|$ at the center of the aperture versus ka for $\alpha = 0°$. The solid curve is $\phi_o = 10°$. The dashed curve is for $\phi_o = 30°$.

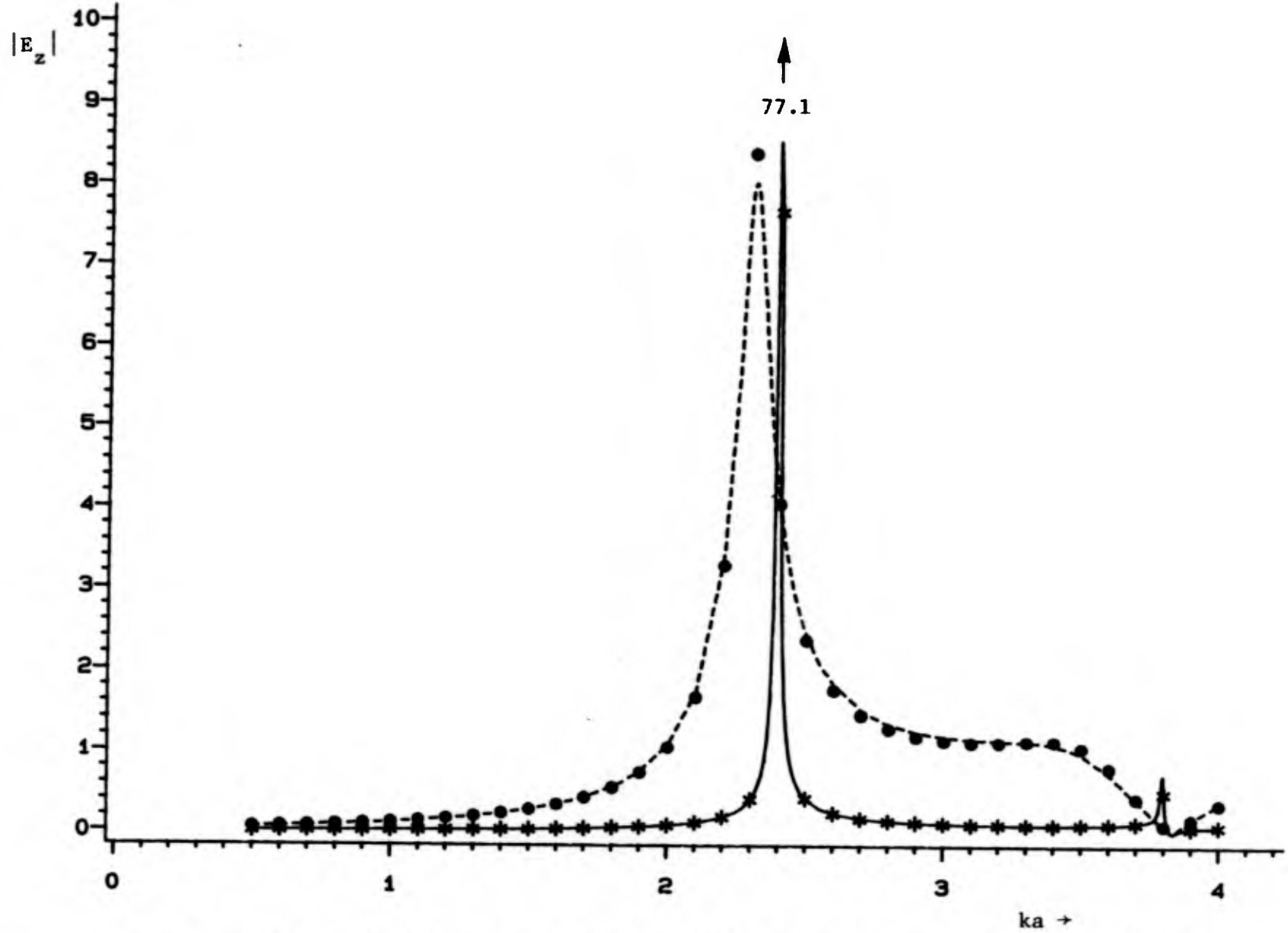

Fig. 14. Field amplitude $|E_z|$ at the center of the cylinder versus ka for $\alpha = 0°$. The solid curve is for $\phi_o = 10°$. The dashed curve is for $\phi_o = 30°$.

of $|E_z|$ for $\phi_o = 10°$. The dashed curve is for $\phi_o = 30°$, and the large dots represent crude values of $|E_z|$ for $\phi_o = 30°$. In Fig. 15, the data of Fig. 14 are plotted on a logarithmic scale. At the value of ka such that $J_o(ka) = 0$, our $|E_z|$ is 3.96 for $\phi_o = 30°$ and 4.06 for $\phi_o = 10°$ whereas (75) gives $|E_z| = 4.07$ at $\rho = 0$. Note that the 10° and 30° curves in Figs. 14 and 15 cross each other at $|E_z| \simeq 4.0$. The $|E_z|$ for $\phi_o = 30°$ in Figs. 14 and 15 agrees with that in [1, Fig. 5] and [2, Figs. 18 and 19]. However, the $|E_z|$ for $\phi_o = 10°$ in Figs. 14 and 15 is noticeably different from that in [1, Fig. 5] and [2, Figs. 18 and 19]. Our $|E_z|$ for $\phi_o = 10°$ has no minimum in the vicinity of ka = 1 and has a deep minimum in the vicinity of ka = 3.8 rather than in the vicinity of ka = 2.4.

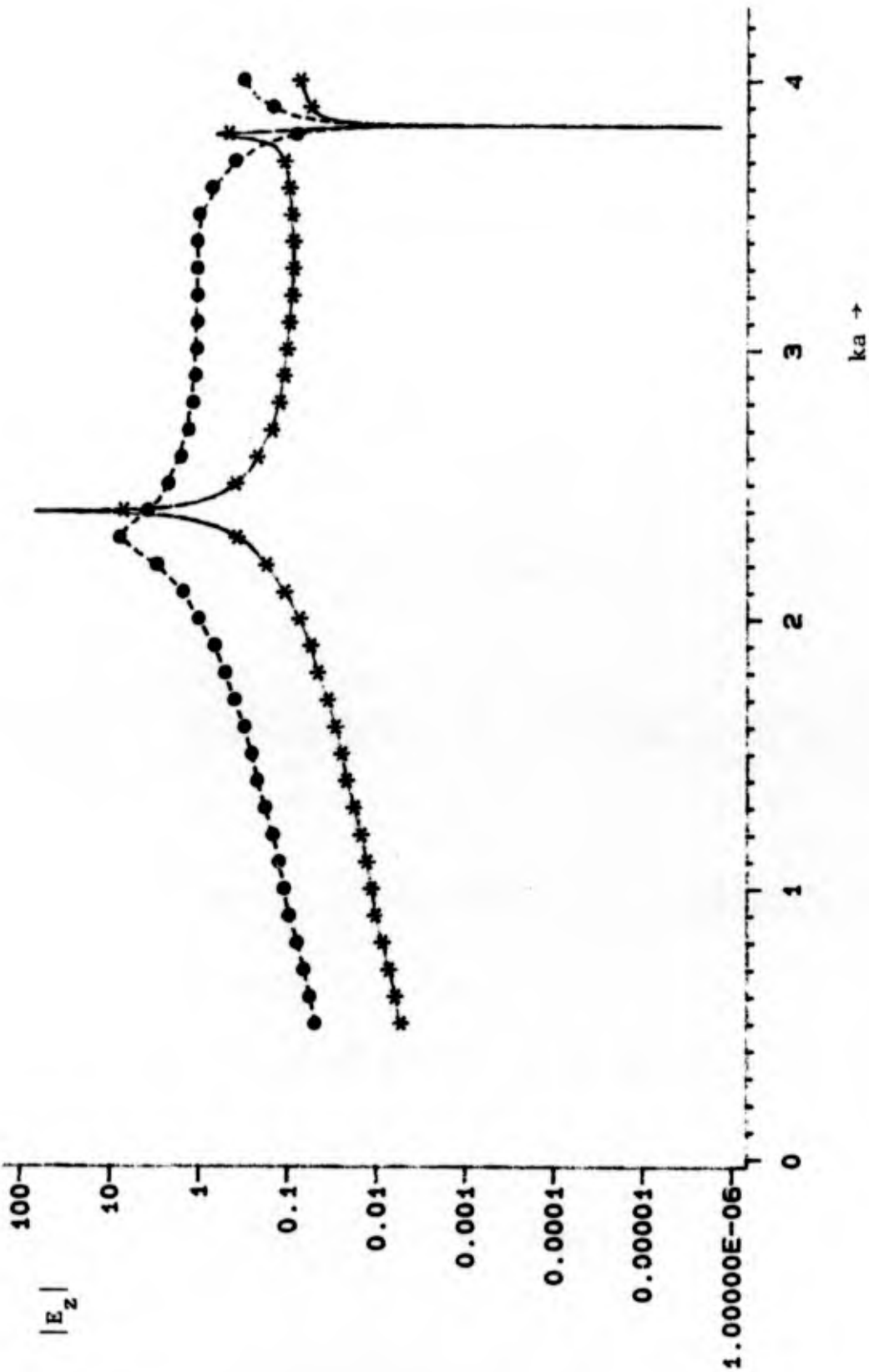

Fig. 15. Field amplitude $|E_z|$ at the center of the cylinder versus ka for $\alpha = 0°$. The solid curve is for $\phi_o = 10°$. The dashed curve is for $\phi_o = 30°$.

APPENDIX A

EVALUATION OF S^e_{jn} AND S^o_{jn}

Changing the variable of integration from ϕ to

$$x = \phi/\phi_o \tag{A-1}$$

in (15) and (27), we obtain

$$S^e_{jn} = \frac{\varepsilon_n \phi_o}{2\pi} \int_{-1}^{1} x^{2j-2} \sqrt{1 - x^2} \cos (bx)\, dx \tag{A-2}$$

$$S^o_{jn} = \frac{\phi_o}{\pi} \int_{-1}^{1} x^{2j-1} \sqrt{1 - x^2} \sin (bx)\, dx \tag{A-3}$$

where

$$b = n\phi_o \tag{A-4}$$

In regard to (A-2) and (A-3), it is known that [16, formulas 3.752(2.) and 3.753(2.)]

$$\int_{-1}^{1} \sqrt{1 - x^2} \cos (bx)\, dx = \frac{\pi J_1(b)}{b} \tag{A-5}$$

and

$$\int_{-1}^{1} \frac{\cos (bx)\, dx}{\sqrt{1 - x^2}} = \pi J_o(b) \tag{A-6}$$

Assuming that $n \neq 0$, comparison of (A-5) with (A-2) gives

$$S^e_{1n} = \frac{J_1(b)}{n} \tag{A-7}$$

Integrating the right-hand side of (A-3) by parts, we obtain

$$S^o_{1n} = \frac{1}{n\pi} \int_{-1}^{1} \cos (bx) \frac{d}{dx} \left(x \sqrt{1 - x^2}\right) dx \tag{A-8}$$

which becomes

$$S^{o}_{1n} = \frac{1}{n\pi} \int_{-1}^{1} [2\sqrt{1 - x^2} - \frac{1}{\sqrt{1 - x^2}}] \cos (bx)\, dx \qquad \text{(A-9)}$$

Formulas (A-5) and (A-6) reduce (A-9) to

$$S^{o}_{1n} = \frac{2J_1(b) - bJ_o(b)}{nb} \qquad \text{(A-10)}$$

Seeking a recurrence relation for S^{e}_{jn} when $n \neq 0$, we use the identity

$$x^{2j-2} = x^{2j-4}(1 - (1-x^2)) \qquad \text{(A-11)}$$

to recast (A-2) as

$$S^{e}_{jn} = S^{e}_{j-1,n} - \frac{\phi_o}{\pi} \int_{-1}^{1} x^{2j-4}(1-x^2)^{3/2} \cos (bx)\, dx \qquad \text{(A-12)}$$

which, upon integration by parts, becomes

$$S^{e}_{jn} = S^{e}_{j-1,n} + \frac{\phi_o}{b\pi} \int_{-1}^{1} \sin (bx) \frac{d}{dx} (x^{2j-4}(1 - x^2)^{3/2})dx \qquad \text{(A-13)}$$

performing the indicated differentiation in (A-13), we obtain the recurrence relation

$$S^{e}_{jn} = S^{e}_{j-1,n} - (\frac{2j-1}{b})\, S^{o}_{j-1,n} + \frac{2(j-2)}{b}\, S^{o}_{j-2,n} \quad , \; j=2,3,\ldots \qquad \text{(A-14)}$$

where the $S^{o}_{j-2,n}$ term is to be omitted when j is 2.

Seeking a recurrence relation for S^{o}_{jn}, we use an identity similar to (A-11) to recast (A-3) as

$$S^{o}_{jn} = S^{o}_{j-1,n} - \frac{\phi_o}{\pi} \int_{-1}^{1} x^{2j-3}\, (1-x^2)^{3/2} \sin (bx)\, dx \qquad \text{(A-15)}$$

An integration by parts changes (A-15) to

$$S^{o}_{jn} = S^{o}_{j-1,n} - \frac{\phi_o}{b\pi} \int_{-1}^{1} \cos(bx) \frac{d}{dx} (x^{2j-3}(1-x^2)^{3/2})dx \qquad \text{(A-16)}$$

Performing the indicated differentiation in (A-16), we obtain the recurrence relation

$$S^{o}_{jn} = S^{o}_{j-1,n} + (\frac{2j}{b}) S^{e}_{jn} - (\frac{2j-3}{b}) S^{e}_{j-1,n}, \quad j=2,3,... \qquad \text{(A-17)}$$

Using (A-14) and (A-17) to recur up from (A-7) and (A-10), we obtain

$$S^{e}_{1n} = \frac{J_1(b)}{n} \qquad \text{(A-18)}$$

$$S^{e}_{2n} = \frac{(b^2-6)\ J_1(b) + 3bJ_o(b)}{nb^2} \qquad \text{(A-19)}$$

$$S^{e}_{3n} = \frac{(b^4-27b^2+120)\ J_1(b) + 6b\ (b^2-10)\ J_o(b)}{nb^4} \qquad \text{(A-20)}$$

$$S^{e}_{4n} = \frac{(b^6-63b^4+1200b^2-5040)\ J_1(b) + 3b(3b^4-95b^2+840)J_o(b)}{nb^6} \qquad \text{(A-21)}$$

$$S^{o}_{1n} = \frac{2J_1(b) - b\ J_o(b)}{nb} \qquad \text{(A-22)}$$

$$S^{o}_{2n} = \frac{(5b^2-24)\ J_1(b) - (b^2-12)b\ J_o(b)}{nb^3} \qquad \text{(A-23)}$$

$$S^{o}_{3n} = \frac{(8b^4-168b^2+720)\ J_1(b) - (b^4-39b^2+360)b\ J_o(b)}{nb^5} \qquad \text{(A-24)}$$

$$S^{o}_{4n} = \frac{(11b^6-537b^4+9720b^2-40320)J_1(b)-(b^6-81b^4+2340b^2-20160)b\ J_o(b)}{nb^7} \qquad \text{(A-25)}$$

Expressions (A-19) - (A-25) become indeterminate as b approaches zero. When $b \leq 2$, we approximate cos (bx) in (A-2) by [17, formula 415.02].

$$\cos(bx) = 1 - \frac{b^2x^2}{2} + \frac{b^4x^4}{24} - \frac{b^6x^6}{720} + \frac{b^8x^8}{40320} - \frac{b^{10}x^{10}}{3628800} \qquad \text{(A-26)}$$

We encounter integrals I_{2j} defined by

$$I_{2j} = \int_{-1}^{1} x^{2j} \sqrt{1 - x^2}\, dx, \quad j = 0,1,2,\ldots \qquad \text{(A-27)}$$

It is evident from [16, formula 3.248(3.)] that

$$I_{2j} = \frac{\pi(2j-1)!!}{(2j+2)!!}, \quad j = 0,1,2,\ldots \qquad \text{(A-28)}$$

where

$$(2j-1)!! = \begin{cases} 1 & , \quad j = 0 \\ 1\cdot 3\cdot 5,\ldots\ 2j-1 & , \quad j \geq 1 \end{cases} \qquad \text{(A-29)}$$

and

$$(2j)!! = 2\cdot 4\cdot 6,\ldots,\ 2j \qquad \text{(A-30)}$$

From (A-28), we obtain

$$\begin{aligned} I_0 &= \pi/2 \\ I_2 &= \pi/8 \\ I_4 &= \pi/16 \\ I_6 &= 5\pi/128 \\ I_8 &= 7\pi/256 \\ I_{10} &= 21\pi/1024 \\ I_{12} &= 33\pi/2048 \\ I_{14} &= 429\pi/32768 \\ I_{16} &= 715\pi/65536 \\ I_{18} &= 2431\pi/262144 \end{aligned} \qquad \text{(A-31)}$$

In view of (A-31), substitution of (A-26) into (A-2) gives

$$S_{1n}^{e} = \frac{\varepsilon_n \phi_o}{4}\left(1 - \frac{b^2}{8} + \frac{b^4}{192} - \frac{b^6}{9216} + \frac{b^8}{737280} - \frac{b^{10}}{88473600}\right) \tag{A-32}$$

$$S_{2n}^{e} = \frac{\varepsilon_n \phi_o}{16}\left(1 - \frac{b^2}{4} + \frac{5b^4}{384} - \frac{7b^6}{23040} + \frac{b^8}{245760} - \frac{11b^{10}}{309657600}\right) \tag{A-33}$$

$$S_{3n}^{e} = \frac{\varepsilon_n \phi_o}{32}\left(1 - \frac{5b^2}{16} + \frac{7b^4}{384} - \frac{7b^6}{15360} + \frac{11b^8}{1720320} - \frac{143b^{10}}{2477260800}\right) \tag{A-34}$$

$$S_{4n}^{e} = \frac{5\varepsilon_n \phi_o}{256}\left(1 - \frac{7b^2}{20} + \frac{7b^4}{320} - \frac{11b^6}{19200} + \frac{143b^8}{17203200} - \frac{143b^{10}}{1857945600}\right) \tag{A-35}$$

When $b \leq 2$, we approximate sin (bx) in (A-3) by [17, formula 415.01].

$$\sin(bx) = bx - \frac{b^3x^3}{6} + \frac{b^5x^5}{120} - \frac{b^7x^7}{5040} + \frac{b^9x^9}{362880} - \frac{b^{11}x^{11}}{39916800} \tag{A-36}$$

We substitute (A-36) into (A-3) and use (A-31) in order to obtain

$$S_{1n}^{o} = \frac{\phi_o b}{8}\left(1 - \frac{b^2}{12} + \frac{b^4}{384} - \frac{b^6}{23040} + \frac{b^8}{2211840} - \frac{b^{10}}{309657600}\right) \tag{A-37}$$

$$S_{2n}^{o} = \frac{\phi_o b}{16}\left(1 - \frac{5b^2}{48} + \frac{7b^4}{1920} - \frac{b^6}{15360} + \frac{11b^8}{15482880} - \frac{13b^{10}}{2477260800}\right) \tag{A-38}$$

$$S_{3n}^{o} = \frac{5\phi_o b}{128}\left(1 - \frac{7b^2}{60} + \frac{7b^4}{1600} - \frac{11b^6}{134400} + \frac{143b^8}{154828800} - \frac{13b^{10}}{1857945600}\right) \tag{A-39}$$

$$S_{4n}^{o} = \frac{7\phi_o b}{256}\left(1 - \frac{b^2}{8} + \frac{11b^4}{2240} - \frac{143b^6}{1505280} + \frac{143b^8}{130056192} - \frac{17b^{10}}{2000864492}\right) \tag{A-40}$$

APPENDIX B

EVALUATION OF F^e_{in} AND F^o_{in}

In this appendix, we obtain expressions for F^e_{in} and F^o_{in} by exact evaluation of the integrals in (43) and (49). Unfortunately, these expressions become indeterminate as $n\phi_o$ approaches zero. For $n\phi_o \leq 2$, we approximate cos $(n\phi)$ and sin $(n\phi)$ by the first 6 terms of their power series and then evaluate the resulting integrals.

Changing the variable of integration from ϕ to

$$x = n\phi \tag{B-1}$$

in (43) and (49), assuming that $n \neq 0$, and taking advantage of the fact that the resulting integrands are even in x, we obtain

$$F^e_{in} = \frac{1}{nb^{2i-2}} \int_0^b x^{2i-2} \cos x \, dx \tag{B-2}$$

and

$$F^o_{in} = \frac{1}{nb^{2i-1}} \int_0^b x^{2i-1} \sin x \, dx \tag{B-3}$$

where

$$b = n\phi_o \tag{B-4}$$

Since the integrals in (B-2) are given by [17, formulas 440.10, 440.12, 440.14, and 440.16], we have

$$F^e_{1n} = \frac{\sin b}{n} \tag{B-5}$$

$$F^e_{2n} = \frac{2b \cos b + (b^2 - 2) \sin b}{nb^2} \tag{B-6}$$

$$F^e_{3n} = \frac{4(b^2 - 6)b \cos b + (b^4 - 12b^2 + 24) \sin b}{nb^4} \tag{B-7}$$

$$F^e_{4n} = \frac{6(b^4 - 20b^2 + 120)b \cos b + (b^6 - 30b^4 + 360b^2 - 720)\sin b}{nb^6} \tag{B-8}$$

Since the integrals in (B-3) are given by [17, formulas 430.11, 430.13, 430.15, and 430.19], we have

$$F^o_{1n} = \frac{\sin b - b \cos b}{nb} \tag{B-9}$$

$$F^o_{2n} = \frac{3(b^2 - 2) \sin b - (b^2 - 6) b \cos b}{nb^3} \tag{B-10}$$

$$F^o_{3n} = \frac{5(b^4 - 12b^2 + 24) \sin b - (b^4 - 20b^2 + 120)b \cos b}{nb^5} \tag{B-11}$$

$$F^o_{4n} = \frac{7(b^6 - 30b^4 + 360b^2 - 720)\sin b - (b^6 - 42b^4 + 840b^2 - 5040)b \cos b}{nb^7} \tag{B-12}$$

Expressions (B-6)-(B-12) become indeterminate as b approaches zero. For $b \leq 2$, we approximate cos x in (B-2) by [17, formula 415.02]

$$\cos x = 1 - \frac{x^2}{2} + \frac{x^4}{24} - \frac{x^6}{720} + \frac{x^8}{40320} - \frac{x^{10}}{3628800} \tag{B-13}$$

and sin x in (B-3) by [17, formula 415.01]

$$\sin x = x - \frac{x^3}{6} + \frac{x^5}{120} - \frac{x^7}{5040} + \frac{x^9}{362880} - \frac{x^{11}}{39916800} \tag{B-14}$$

and use

$$\int_0^b x^{2i} dx = \frac{b^{2i+1}}{2i+1} \tag{B-15}$$

to obtain

$$F^e_{in} = \phi_o\left(\frac{1}{2i-1} - \frac{b^2}{2(2i+1)} + \frac{b^4}{24(2i+3)} - \frac{b^6}{720(2i+5)} + \frac{b^8}{40320(2i+7)} - \frac{b^{10}}{3628800(2i+9)}\right) \tag{B-16}$$

$$F^o_{in} = b\phi_o\left(\frac{1}{2i+1} - \frac{b^2}{6(2i+3)} + \frac{b^4}{120(2i+5)} - \frac{b^6}{5040(2i+7)} + \frac{b^8}{362880(2i+9)} - \frac{b^{10}}{39916800(2i+11)}\right) \tag{B-17}$$

Letting i run from 1 to 4 in (B-16) and (B-17), we have

$$F^e_{1n} = \phi_o\left(1 - \frac{b^2}{6} + \frac{b^4}{120} - \frac{b^6}{5040} + \frac{b^8}{362880} - \frac{b^{10}}{39916800}\right) \tag{B-18}$$

$$F^e_{2n} = \frac{\phi_o}{3}\left(1 - \frac{3b^2}{10} + \frac{b^4}{56} - \frac{b^6}{2160} + \frac{b^8}{147840} - \frac{b^{10}}{15724800}\right) \tag{B-19}$$

$$F^e_{3n} = \frac{\phi_o}{5}\left(1 - \frac{5b^2}{14} + \frac{5b^4}{216} - \frac{b^6}{1584} + \frac{b^8}{104832} - \frac{b^{10}}{10886400}\right) \tag{B-20}$$

$$F^e_{4n} = \frac{\phi_o}{7}\left(1 - \frac{7b^2}{18} + \frac{7b^4}{264} - \frac{7b^6}{9360} + \frac{b^8}{86400} - \frac{b^{10}}{8812800}\right) \tag{B-21}$$

$$F^o_{1n} = \frac{\phi_o b}{3}\left(1 - \frac{b^2}{10} + \frac{b^4}{280} - \frac{b^6}{15120} + \frac{b^8}{1330560} - \frac{b^{10}}{172972800}\right) \tag{B-22}$$

$$F^o_{2n} = \frac{\phi_o b}{5}\left(1 - \frac{5b^2}{42} + \frac{b^4}{216} - \frac{b^6}{11088} + \frac{b^8}{943488} - \frac{b^{10}}{119750400}\right) \tag{B-23}$$

$$F^o_{3n} = \frac{\phi_o b}{7}\left(1 - \frac{7b^2}{54} + \frac{7b^4}{1320} - \frac{b^6}{9360} + \frac{b^8}{777600} - \frac{b^{10}}{96940800}\right. \tag{B-24}$$

$$F^o_{4n} = \frac{\phi_o b}{9}\left(1 - \frac{3b^2}{22} + \frac{3b^4}{520} - \frac{b^6}{8400} + \frac{b^8}{685440} - \frac{b^{10}}{84268800}\right) \tag{B-25}$$

REFERENCES

[1] T.B.A. Senior, "Electromagnetic Field Penetration into a cylindrical Cavity," IEEE Trans. Electromagn. Compat., vol. EMC-18, May 1976.

[2] T.B.A. Senior, "Field Penetration into a Cylindrical Cavity," Report 012643-2-T, The University of Michigan Radiation Lab., Ann Arbor, MI, Jan. 1975.

[3] J. R. Mautz, X. Yuan, and R. F. Harrington, "Electromagnetic Scattering from a Slotted TM Cylindrical Conductor by the Pseudo-Image Method," Technical Report SYRU/DECE/TR-85/3, Department of Electrical and Computer Engineering, Syracuse University, Syracuse, NY 13244, Sept. 1985.

[4] J. R. Mautz and R. F. Harrington, "Computer Programs for Electromagnetic Scattering from a Slotted TM Cylindrical Conductor by the Pseudo-Image Method," Technical Report SYRU/DECE/TR-85/5, Department of Electrical and Computer Engineering, Syracuse University, Syracuse, NY 13244, Nov. 1985.

[5] D. R. Rhodes, "Theory of Axially Slitted Circular and Elliptic Cylinder Antennas," J. Appl. Phys., vol. 21, pp. 1181-1188, Nov. 1950.

[6] Y. Hayashi, "A Singular Integral Equation Approach to Electromagnetic Fields for Circular Boundaries with Slots," Appl. Sci. Res., vol. B12, pp. 331-359, 1965.

[7] V. N. Koshparënok and V. P. Shestopalov, "Diffraction of a Plane Electromagnetic Wave by a Circular Cylinder with a Longitudinal Slot," U.S.S.R. Comp. Math. and Math. Phys., vol. 11, pp. 222-243, 1971.

[8] W. A. Johnson and R. W. Ziolkowski, "The Scattering of an H-Polarized Plane Wave from an Axially Slotted Infinite Cylinder: A Dual Series Approach," Radio Science, vol. 19, pp. 275-291, Jan.-Feb. 1984.

[9] R. W. Ziolkowski, W. A. Johnson, and K. F. Casey, "Applications of Riemann-Hilbert Problem Techniques to Electromagnetic Coupling through Apertures," Radio Science, Vol. 19, pp. 1425-1431, Nov.-Dec. 1984.

[10] R. W. Ziolkowski, "n-Series Problems and the Coupling of Electromagnetic Waves to Apertures: A Riemann-Hilbert Approach," SIAM J. Math. Anal., vol. 16, pp. 358-378, March 1985.

[11] R. F. Harrington and J. R. Mautz, "A Generalized Network Formulation for Aperture Problems," IEEE Trans. Antennas Propagat., vol. AP-24, pp. 870-873, Nov. 1976.

[12] C. M. Butler and D. R. Wilton, "General Analysis of Narrow Strips and Slots," IEEE Trans. Antennas Propagat., vol. AP-28, pp. 42-48, Jan. 1980.

[13] R. F. Harrington, Time-Harmonic Electromagnetic Fields, McGraw-Hill, New York, 1961.

[14] P. M. Morse and H. Feshbach, Methods of Theoretical Physics, Part II, McGraw-Hill, New York, 1953.

[15] X. Yuan, R. F. Harrington, and J. R. Mautz, "The Pseudo-Image Method for Computing Electromagnetic Field Penetration into a Cylindrical Cavity, TM Case," Report SYRU/DECE/TR-86/1, Department of Electrical and Computer Engineering, Syracuse University, Syracuse, NY 13210, May 1986.

[16] I. S. Gradshteyn and I. M. Ryzhik, Tables of Integrals, Series, and Products, Academic Press, New York, 1965.

[17] H. B. Dwight, Tables of Integrals and Other Mathematical Data, Macmillan, New York, 1961.